TWO-BODY REGGE AMPLITUDES AS HOLOGRAMS*

Robi Peschanski

Institut de Physique Théorique, CEA/Saclay
91191 Gif-sur-Yvette cedex, France†
robi.peschanski@cea.fr

(Received November 28, 2011)

A conjecture, in 1999–2001 papers by R. Janik and the author, concerns the holographic description of two-body amplitudes at high energy in terms of AdS/CFT correspondence and more general Gauge/Gravity duality. It states that those amplitudes are related to the *helicoidal* geometry in the Euclidean version of the gravity duals. The purpose of this paper is a test of this conjecture and the subsequent derivation of the *Regge behaviour* of these amplitudes using the recent progresses in AdS/CFT correspondence and its extension to non-conformal Gauge/Gravity duality. In Section 1, we provide a test of the conjecture by comparing, after analytic continuation from Euclidean to Minkowski space-time, the prediction for the *logarithmic* Regge trajectory for elastic two-quark amplitude with the one obtained from the Alday–Maldacena 2007 solution for the two-gluon amplitude. In Section 2, we derive the high-energy quark–antiquark exchange (Reggeon) amplitude in the context of Gauge/Gravity duality for a generic confining case. By a suitable analytic continuation, we confirm the prediction of *linear* Regge trajectories obtained in the original papers and derive new results on the exchanged quark mass dependence of the reggeon amplitude. The new material contained in the paper comes from a collaboration with Matteo Giordano and Shigenori Seki.

DOI:10.5506/APhysPolB.42.2751
PACS numbers: 12.38–t, 12.38.Lg, 12.38.Aw

* Presented at the LI Cracow School of Theoretical Physics "Soft Side of the LHC", Zakopane, Poland, June 11–19, 2011.

† URA 2306, unité de recherche associée au CNRS.

1. The helicoid conjecture and its AdS/CFT test

1.1. Introduction: Regge amplitudes and minimal surfaces in Gauge/Gravity duality

Our general goal is to make use of the AdS/CFT (for the conformal $\mathcal{N}=4$ super Yang–Mills (SYM) gauge theory) and Gauge/Gravity duality (for QCD-like confining gauge theories) in order to study the high-energy behaviour of soft two-body scattering amplitudes at strong coupling.

This problem has a quite remarkable historic role [1] since it may be considered as giving the initial motivation for building a quantum string theory in general. This comes from the problem of building "dual" amplitudes for strong interactions in which the same two-body amplitude can be described in two ways. From the low-energy side by an infinite summation of s-channel resonances or, from the high-energy side by a summation of t-channel Regge pole contributions. One writes

$$A_{R,P}\left(s,t=-q^2\right) \equiv \left(\frac{s}{s_0}\right)^{\alpha(t)} \beta(t) + \sum_{i=1}^{\infty} \left(\frac{s}{s_0}\right)^{\alpha_i(t)} \beta^i(t)\,, \tag{1}$$

where $\alpha_i(t)$, are the so-called Regge trajectories and $\beta_i(t)$, the Regge residue. A hierarchy

$$\alpha(t) > \alpha_1(t) > \cdots \alpha_i(t) > \alpha_{i+1}(t) > \cdots$$

is implicitly assumed, showing that the high-energy amplitude when $s/s_0 \gg 1$ is dominated by the leading Regge trajectory $\alpha(t)$. In (1), the subscripts R, P distinguish two types of trajectories depending on the exchanged quantum numbers, namely the *Reggeons*, with non-vacuum exchange and the *Pomeron*, characterised by vacuum quantum number exchanges.

A thorough study, which overall took more than 10 years during the sixties–seventies, revealed that Eq. (1) has its formal foundation in terms of a string theory, which was thus built starting from these "dual" Regge formulation. In string theoretical terms, the Reggeon-based $A_R(s,t=-q^2)$, known as the Veneziano amplitude corresponds to the exchange of an open string, see Fig. 1 (left), while the Pomeron-based one $A_P(s,t=-q^2)$, see Fig. 1 (right), corresponds to a closed string exchange.

However, in the same time when a solid construction string theory was on the way, soon appeared important questions and obstructions to the derivation of high-energy amplitudes from string theory in a d-dimensional Minkowski background. Indeed, a string theory is not consistent with the phenomenological requirements of strong interaction amplitudes in physical 4-dimensional Minkowski space-time: It appears to require 26 dimensions (for the bosonic string) or 10 dimensions (for the superstring including fermions). For those critical dimensions, one gets zero-mass on-shell states in

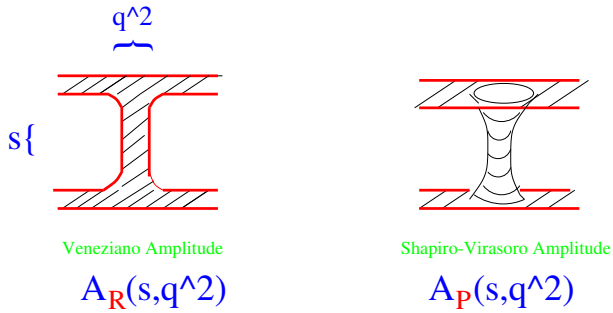

Fig. 1. Two-body amplitudes in terms of tree-level string diagrams. Left: Open string exchange; Right: Closed string exchange.

the spectrum, which are identified with vector and graviton fields. Replacing the QCD scale by the Planck scale, a consistent string theory on higher dimensional space-time is more appropriate, for the unification of gauge field theories with gravity. Hence for some time, the strong-interaction/string theory connection was abandoned.

The change came more recently when a new string scenario, connecting gauge theories at strong coupling to string theories on curved backgrounds, appeared. It is the now famous AdS/CFT correspondence and its generalisation in terms of Gauge/Gravity duality [2].

Before giving more details on this scenario, we already mention that our aim is to use this scenario in order to come back, in some sense, to the original problem, and thus to explore the high-energy energy behaviour of two-body amplitudes (1) from the point-of-view of Gauge/Gravity duality. We divide our study in two parts corresponding to the following questions:

- Can we understand the Regge behaviour for two-body amplitudes of conformal $\mathcal{N}=4$ gauge field theory using the well-established AdS/CFT correspondence?

- Can we derive from Gauge/Gravity duality the Regge behaviour for a non-conformal, confining, gauge field theory, which would be as similar as possible to QCD at strong coupling?

In the initial papers [3, 4, 5], the holographic description of two-body high-energy amplitudes, following the Gauge/Gravity duality approach, has been based on the correspondence between Wilson loop expectation values in the gauge field theory and minimal surfaces in the gravity dual. This relation may be formally written (in some qualitative way here, more precise definition to be seen further on)

$$\left\langle \exp iP \int\limits_{C} \vec{A} \cdot \vec{dl} \right\rangle = \int\limits_{\Sigma} \exp -\frac{\text{Area}(\Sigma)}{\alpha'} \approx \exp -\frac{\text{Min. Area}}{\alpha'} \times \text{Fluctuations}\,, \tag{2}$$

where the Wilson loop contour C is drawn on the 4-dimensional physical boundary space, and is the frontier of the 5-dimensional *Wilson surface* Σ whose minimal area gives the leading holographic evaluation of the Wilson loop expectation value (the fluctuation correction term is expected to be arising from the first-order fluctuations of the integral in (2) around the minimal surface solution). In the simple case of parallel Wilson lines, this correspondence is described in Fig. 2. The problem thus amounts to solve the minimal surface problem for a given frontier defined by the Wilson loop. For a confining theory (Fig. 2 (left)), it has been noticed in [4] that this is related to the flat space problem on the near-horizon. For a conformal background (Fig. 2 (left)), the minimal surface problem has to be formulated using the appropriate gravitational metric, *e.g.* AdS_5 in the case of $\mathcal{N} = 4$ SYM Wilson loops. Note that we will consider the correspondence either for Minkowski or Euclidean boundary spaces. In the latter case, an analytic continuation from Euclidean to Minkowski is required in order to get the result for the physical amplitudes.

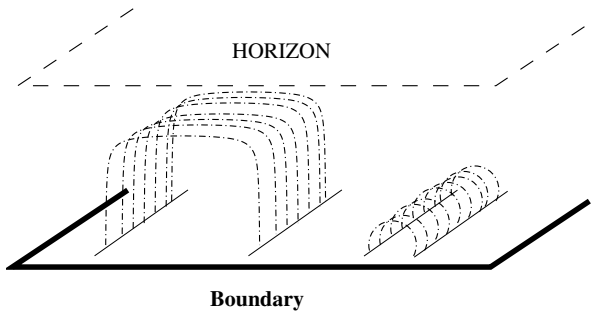

Fig. 2. Wilson-loop/Minimal-surface correspondence. Left: Confining background $\sim$ QCD; Right: Non-confining background $\sim \mathcal{N} = 4$ SYM.

The main idea for the holographic description of high-energy amplitudes, as proposed in Refs. [3, 4, 5] was to make use of the *eikonal* approximation well-known in various applications of field theory to give a good description of two-body scattering processes at high energies through analytic continuation in Euclidean space. The use of Euclidean space was motivated by the relation between specific Wilson loops to amplitudes, and thus by the possibility to use in a quite direct way the Wilson-loop/Minimal-surface correspondence.

As a direct application, the eikonal configuration suggests that an high-energy two-body amplitude has something to do with the *Helicoidal Geometry* in the 5-dimensional gravity background. Indeed, consider for instance the eikonal configuration of two-quark scattering in Euclidean coordinate space, see Fig. 3 (a). The physical amplitude in Minkowskian impact-parameter space is defined as

$$a\left(L=|\vec{b}|,\chi\right)\equiv\frac{i}{2s}\int\frac{d^2\vec{q}}{(2\pi)^2}e^{-i\vec{q}\cdot\vec{b}}\;A_{\mathcal{P}}(s,t)\,, \tag{3}$$

where the impact-parameter variable is $\vec{b}$ and $\chi=\log s$, the total rapidity. Then the correspondence writes [3]

$$\tilde{a}\,(L,\theta\to-i\chi,T)=\mathcal{Z}^{-1}\int\limits_{\mathcal{C}}\langle W[\mathcal{C}]\rangle\sim\exp\left\{-\frac{\mathcal{A}_{\text{Helicoid}}}{\alpha'}\right\}, \tag{4}$$

where $\tilde{a}(L=|\vec{b}|,\theta)$ is the impact-parameter "amplitude" in Euclidean position space, defined replacing the rapidity χ by using the angle θ between the two quark straight lines which characterise the eikonal approximation. Z is an (infinite) renormalisation constant and T a long-distance cut-off (these constants are related to the important question of divergences which will be discussed later on). The physical impact parameter amplitude is then obtained, after proper renormalisation, through analytic continuation from Euclidean to Minkowskian impact-parameter space $\tilde{a}(L,\theta\to-i\chi,T)\to a(L=|\vec{b}|,\chi)$.

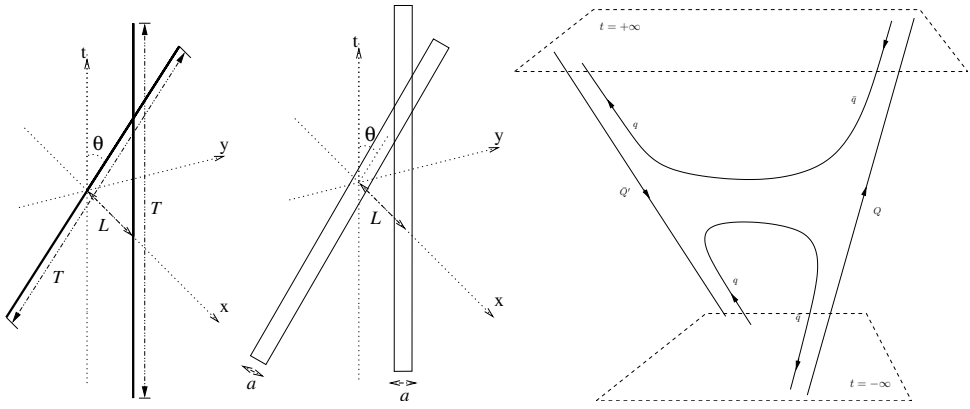

(a) qq elastic
Infinite Wilson loop
Single helicoid
Divergences

(b) dipole elastic
Wilson loop Correlator
"Double-sheeted" helicoid
Approximate geometry

(c) $q\bar{q}$ exchange
Finite "twisted" loop
Wilson lines on helicoid
Floating Boundaries

Fig. 3. Boundary Wilson loops in Euclidean coordinate space.

In flat space metric, the helicoid is represented in Fig. 4 for illustration, its area is well-known, and writes

$$\text{Min. Area}\,(L,\theta,T) = LT\sqrt{1+\frac{T^2\theta^2}{L^2}} + \frac{L^2}{2\theta}\log\left\{\frac{\sqrt{1+\frac{T^2\theta^2}{L^2}}+\theta\frac{T}{L}}{\sqrt{1+\frac{T^2\theta^2}{L^2}}-\theta\frac{T}{L}}\right\}. \quad (5)$$

Note, however, that this area is strictly speaking the minimal one only when $T \to \infty$, but then obviously Min. Area $\to \infty$, also. Hence, the problem of divergences should be faced, as we shall see in detail for the $\mathcal{N} = 4$ SYM case, where the same problem appears.

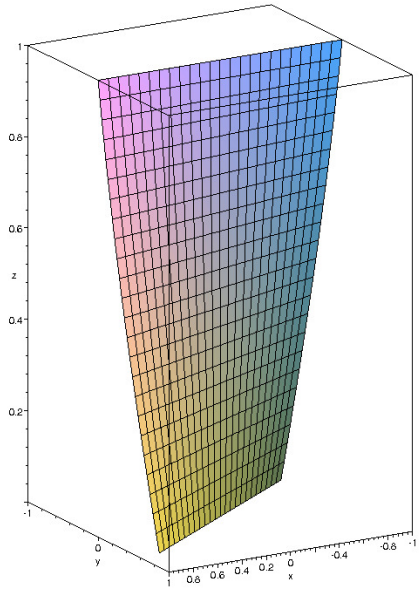

Fig. 4. Helicoid geometry in flat space.

The similar formula in AdS space is not known. Hence, the use of nearly flat space geometry (as in Fig. 2 (left)) will be easier, but approximate, while the AdS geometry, for the better known AdS/CFT correspondence will be more delicate. It would correspond to a "generalised helicoid" geometry in AdS space, *i.e.* the minimal surface with infinitely long straight lines at the boundary. We will deal with each case in the paper.

In Fig. 3, we have reproduced the main Wilson loop configurations which were introduced and discussed in Refs. [3, 4, 5]. Fig. 3 (a) corresponds to quark–quark scattering, which has the simplest holographic geometry, since it corresponds to the single helicoid. However, it suffers from divergence

problems and thus requires a renormalisation. This will be dealt with in detail for the conformal case in the following of Section 1. Fig. 3 (b) concerns elastic dipole scattering (*i.e.* the Pomeron amplitude $A_{\mathcal{P}}$), and is expressed in terms of Wilson loop correlators. Being colourless, the dipole is not expected to give rise to divergences, but the minimal geometry is not analytically known. A "double-sheeted" helicoid has been used as an approximation for the confining case [4]. Finally, Fig. 3 (c) is for the Reggeon amplitude $A_{\mathcal{R}}$, corresponding to a single Wilson loop with partially floating boundaries [5]. We will examine this configuration for the confining geometry in Section 2.

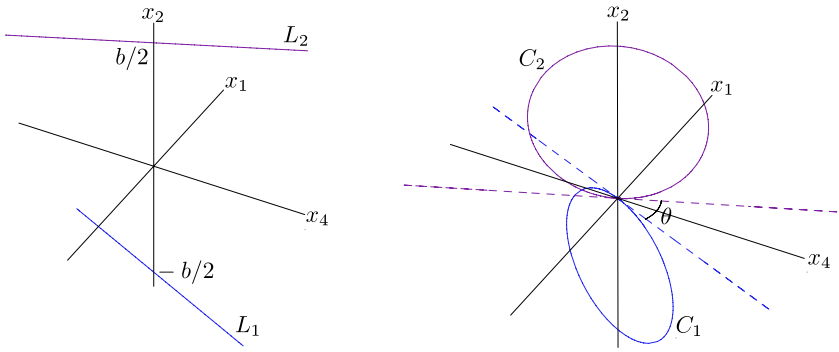

Fig. 5. Boundary for the "generalised helicoid" in the AdS_5 metrics. Left: Initial eikonal geometry; Right: Conformal transform.

1.2. AdS/CFT and $\mathcal{N} = 4$ SYM two-quark scattering amplitude in the eikonal approach

As discussed in the previous section, one starts with the minimal surface for the qq amplitude in the eikonal approach which is a "generalised helicoid" in the AdS_5 metrics (or in short, "AdS_5 helicoid"), *e.g.* the minimal surface with infinite straight lines at the Euclidean boundary, see Fig. 3 (a). The analytic solution for such a minimal surface problem is not yet known. As found in the Ref. [6], a solution is obtained through a conformal transform of the AdS_5 helicoid. Indeed, by the conformal 5-dimensional inversion w.r.t. the origin of axes along the impact-parameter vector in Fig. 5, left, namely

$$x_\mu \to \frac{x_\mu}{|x_\mu|^2 + z^2}\,, \qquad z \to \frac{z}{|x_\mu|^2 + z^2}\,, \tag{6}$$

one obtains a new equivalent minimal surface problem, with two coincident circles, see Fig. 5, right. The key remark of [6] is that the regularised minimal area of the new configuration is dominated by a cusp, which allows for a determination of the leading term of the corresponding high-energy amplitude.

Formally, the minimal area writes

$$A^{\rm quark}_{\theta,b} = \frac{\sqrt{\lambda}}{2\pi}\int d\tau d\sigma \frac{1}{z^2}\sqrt{\det\left(\delta_{\mu\nu}\partial_a x^\mu \partial_b x^\nu + \partial_a z \partial_b z\right)} \equiv \int d\tau d\sigma \mathcal{L} \qquad (7)$$

with the boundary lines at $z = 0$ is expected to be infinite due to IR divergences (the quantity $A^{\rm quark}$ is also UV divergent due to the behaviour of the metric near the boundary $z = 0$. However, the UV divergence is cancelled by the normalisation factor, see the discussion in [6]). In order to regularise the IR divergences, we limit the range of τ to $\tau \in [-T, T]$, understanding that it has to be imposed in the computation of the area, and not in the determination of the minimal surface. The regularised (and UV-subtracted) area of the surface minimising the functional (7) is therefore a function $A^{\rm quark}_{\rm minimal}(\theta, b, T)$, which has now to be determined.

Let us split the IR-regularised, UV-subtracted area functional evaluated on the minimal surface in the inverted coordinates by introducing an intermediate time scale ρ

$$A^{\rm quark}_{\rm min}(\theta, b, T) = A^{\rm quark}_{\rm fin}(\theta, b, \rho) + A^{\rm quark}_{\rm div}(\theta, b, T, \rho)\,, \qquad (8)$$

$$A^{\rm quark}_{\rm fin}(\theta, b, \rho) = \int_{-\rho}^{\rho} d\tau \int_{-b/2}^{b/2} d\sigma\, \mathcal{L}\,, \qquad (9)$$

$$A^{\rm quark}_{\rm div}(\theta, b, T, \rho) = \left(\int_{-T}^{-\rho} + \int_{\rho}^{T}\right) d\tau \int_{-b/2}^{b/2} d\sigma\, \mathcal{L}\,. \qquad (10)$$

It is well-known that when the cut-off $T \to \infty$, the cusps of the new geometrical boundary defined in Fig. 5, right provide a logarithmic divergence in the area functional (8). By introducing an intermediate scale ρ, which is kept fixed in the limit $T \to \infty$, we are able to separate the divergent contribution (10), which will be dominated by the cusp, from a regular, finite part (9), see Fig. 6. The scale ρ is chosen to be large with respect to b (and thus, after inversion, ρ^{-1} is small compared to the circle diameter in Fig. 5, right, but it is otherwise arbitrary. Using conformal invariance, exploiting the known properties of Wilson loop expectation values, and imposing the independence of the cusp dominance w.r.t. the arbitrary intermediate scale ρ we find [6] finally the expression

$$A^{\rm quark}_{\rm div}(\theta, b, T) = 2\Gamma^{\rm E}_{\rm cusp}(\pi - \theta)\log\frac{b}{T} + \Psi_{\rm E}(\theta) + o\left(T^0\right)\,, \qquad (11)$$

where $\Gamma^{\rm E}_{\rm cusp}(\Omega)$ is a known function for Euclidean angle $0 < \Omega < \pi$ calculated in [7], and where the function $\Psi_{\rm E}(\theta)$ remains to be determined. Note

that the form of equation (11) satisfies the general requirement from conformal invariance [3]. The factor 2 in (11) is due to the fact that there are two cusp contributions. We also notice that the cusp term in Eq. (11) comes only from the contribution of the region around the contact point of the two circles, which is related by inversion to the region at infinity of the two straight lines. In other words, the b, T-dependent term is determined only by the initial and final data of quarks, and this reflects well the link between the eikonal approximation and the dominance of the cusps.

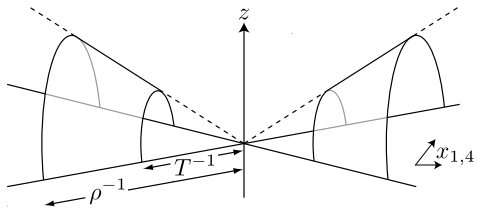

Fig. 6. The contribution to $A_{\rm div}^{\rm quark}(\theta, b, T, \rho)$ of the two cusps with angle θ at the origin.

On the other hand, the function $\Psi_{\rm E}(\theta)$ in Eq. (11) remains to be determined, which would require the exact solution of the minimal surface problem, which is not available at the moment. However, it is possible to go further and determine an interesting approximation by using a "generalised helicoid" ansatz [3]. It amounts to find a refined estimate of the intermediate scale ρ, isolating more precisely the (truncated) cusp contribution. Indeed, we can look for ρ to be not an arbitrary "external" scale, but the one determined by the exact solution of the minimal surface problem, that separates the region, where the surface is well approximated by a cusp solution from the rest.

Since one does not know yet the minimal surface corresponding to the boundaries of Fig. 3, a simple scheme has been introduced in Ref. [3], where the following ansatz for the "generalised helicoid" is assumed in order to find a controllable approximation of the minimal solution, namely

$$x_1 = \tau \sin\frac{\theta\sigma}{b}\,, \qquad x_2 = \sigma\,, \qquad x_3 = 0\,, \qquad x_4 = \tau\cos\frac{\theta\sigma}{b}\,, \qquad z = z(\tau,\sigma)\,. \tag{12}$$

The world-sheet coordinates τ, σ are in the range, $\tau \in [-\infty, \infty]$ and $\sigma \in [-b/2, b/2]$. Using this ansatz, the regularised area functional (8) becomes

$$A_{\rm min}^{\rm quark}(\pi-\theta, b, T) = \frac{\sqrt{\lambda}}{2\pi}\int\limits_{-T}^{+T} d\tau \int\limits_{-b/2}^{+b/2} d\sigma \frac{1}{z^2}\sqrt{\left(1+\frac{\tau^2\theta^2}{b^2}\right)\left(1+(\partial_\tau z)^2\right)+(\partial_\sigma z)^2}\,, \tag{13}$$

where the IR cutoff parameter T is introduced, as explained above.

We remark here that the ansatz (12) is appropriate for quark–antiquark scattering rather than for quark–quark scattering. The reason is that if we want an orientable surface, the two straight-lines which form the boundary of the helicoid, see Fig. 5, left, have to be travelled in opposite directions, if the surface performs a twist of angle θ. On the other hand, if they are travelled in the same direction in order to obtain an orientable surface, the helicoid has to perform a twist of angle $\pi - \theta$. For this reason, we have denoted as $A_{\rm min}^{\rm quark}(\pi - \theta, b)$ the area functional in Eq. (13). Nevertheless, the geometrical problem to be solved in Euclidean space is the same for quark–quark and quark–antiquark scattering. The difference between the two cases lies in the specific analytic continuation which one has to make in order to obtain finally the physical amplitude in Minkowski space-time.

Following Ref. [3], we make the change of variables

$$\sigma' = \sigma\sqrt{1+\left(\frac{\theta\tau}{b}\right)^2}\,, \qquad z'(\tau,\sigma') \equiv z(\tau,\sigma(\tau,\sigma')) \tag{14}$$

which leads to the following expression for the area functional,

$$A_{\rm min}^{\rm quark}(\pi-\theta,b,T) = \frac{\sqrt{\lambda}}{2\pi}\int_{-T}^{T} d\tau \int_{-\frac{b}{2}\sqrt{1+\left(\frac{\theta\tau}{b}\right)^2}}^{\frac{b}{2}\sqrt{1+\left(\frac{\theta\tau}{b}\right)^2}} d\sigma$$
$$\times\frac{1}{z^2}\sqrt{1+(\partial_\sigma z)^2+\left(\partial_\tau z+\frac{\left(\frac{\theta\tau}{b}\right)\left(\frac{\theta\sigma}{b}\right)}{1+\left(\frac{\theta\tau}{b}\right)^2}\,\partial_\sigma z\right)^2}\,, \tag{15}$$

where we have dropped the primes for simplicity.

It can be realized that, written in the form (15), the "generalised helicoid" ansätz admits interesting approximate while explicit solutions for both the large τ regions (also, for the small τ region, but it is not relevant for high energy, see [6]). Considering $\theta\tau/b \gg 1$ the area functional simplifies to

$$A_{\rm min}^{\rm quark}(\pi-\theta,b,T)\big|_{{\rm large}\,\tau} = \frac{\sqrt{\lambda}}{2\pi}\left(\int_{-T}^{-\Lambda\frac{b}{\theta}} + \int_{\Lambda\frac{b}{\theta}}^{T}\right) d\tau \int_{-\frac{\theta|\tau|}{2}}^{\frac{\theta|\tau|}{2}} d\sigma$$
$$\times\frac{1}{z^2}\sqrt{1+(\partial_\sigma z)^2+\left(\partial_\tau z+\frac{\sigma}{\tau}\partial_\sigma z\right)^2}\,, \tag{16}$$

where Λ is some large number. Away from the boundary where $|\sigma/\tau|$ is

small, Eq. (16) can be further approximated as

$$A^{\text{quark}}_{\text{min}}(\pi-\theta,b,T)\big|_{\text{large}\,\tau}=\frac{\sqrt{\lambda}}{2\pi}\left(\int_{-T}^{-\Lambda\frac{b}{\theta}}+\int_{\Lambda\frac{b}{\theta}}^{T}\right)d\tau\int_{-\frac{\theta|\tau|}{2}}^{\frac{\theta|\tau|}{2}}d\sigma$$
$$\times\frac{1}{z^2}\sqrt{1+(\partial_\sigma z)^2+(\partial_\tau z)^2}\,. \tag{17}$$

We have then to deal with a minimal surface with planar boundary, which consists of two segments of straight lines at an angle θ, with $|\tau|\in[\Lambda b/\theta,T]$. The solution is seen to be made up of two parts, each corresponding to a piece of the solution for a cusp of angle θ (*cf.* Fig. 6), and the resulting area is

$$A^{\text{quark}}_{\text{min}}(\pi-\theta,b,T)\big|_{\text{large}\,\tau}=-2\Gamma^{\text{E}}_{\text{cusp}}(\theta)\log\frac{T}{\Lambda b/\theta}=2\Gamma^{\text{E}}_{\text{cusp}}(\theta)\left(\log\frac{b}{T}+\log\frac{\Lambda}{\theta}\right). \tag{18}$$

This result is in agreement with the form (11) for the minimal area, and moreover allows to determine the "natural" choice of a θ-dependent scale $\rho\sim\Lambda b/\theta$, introduced in Eq. (8), which separates the near-cusp region from the rest in the inverted coordinates. Indeed, up to the constant Λ, whose precise value cannot be determined at the present stage, we have that $\rho\propto b/\theta$.

Finally, remark Eq. (18) gives an estimate of the function $\Psi_{\text{E}}(\theta)$ in Eq. (11)

$$\Psi_{\text{E}}(\theta)\sim 2\Gamma^{\text{E}}_{\text{cusp}}(\theta)\log\frac{\Lambda}{\theta}\,, \tag{19}$$

up to possible contributions from the intermediate region $(\tau\theta/b)\in[\delta,\Lambda]$. In a sense, the constant Λ stands for our remaining ignorance about the b,T-independent term $\Psi_{\text{E}}(\theta)$, *i.e.* of the analytic form of the generalised helicoid in AdS geometry.

1.3. Regge behaviour of the two-gluon $\mathcal{N}=4$ SYM amplitude

The two-gluon scattering amplitude in $\mathcal{N}=4$ SYM at strong coupling has been evaluated in Ref. [8], making use of the AdS/CFT correspondence, by computing the area of a corresponding minimal surface. In the dual gravity theory, which is defined in $\text{AdS}_5\times\text{S}^5$, the gluon–gluon scattering amplitude is mapped into the scattering amplitude of four open strings. In turn, the string amplitude is obtained by determining a minimal surface, corresponding to a classical string solution for the Nambu–Goto action. This minimal surface lives in the AdS_5 background, whose metrics parameterises

the *position space*. In Ref. [8] one finds the minimal surface in *momentum space*, rather than directly in the position space. The momentum space is obtained from the position space by means of a T-duality transformation.

In the momentum space, the boundary of the minimal surface corresponding to the two-gluon elastic amplitude is given by the closed sequence of four light-like segments $2\pi k_i$, where the gluons carry momentum k_i, $i=1$–4. The sequences are closed because of momentum conservation, see Fig. 7. The area needs to be regularised for an infra-red divergence, since the min-

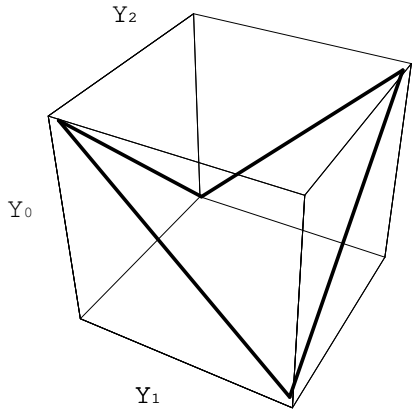

Fig. 7. Minimal-surface's boundary for the two-gluon amplitude. $\{r, Y_i\}$ $i=0-3$ are defined as the coordinate system in the T-dual of ADS_5, see [8].

imal surface, since the light-like segments lie on a D-brane at $r = r_{\rm IR}$ near 0^+, where r is the fifth coordinate in the T-dual space. Such a D-brane acts as a regulator for the IR divergencies of the two-gluon–gluon scattering amplitude, which has to be removed by sending $z_{\rm IR} \to \infty$, *i.e.*, $r_{\rm IR} \to 0$, at the end of the calculation. In Ref. [8] a different but equivalent regularisation has been used, and leads to the following regularised amplitude

$$A(s,t) = \exp\left[2iS_{\rm div}(s) + 2iS_{\rm div}(t) + \frac{\sqrt{\lambda}}{8\pi}\left(\log\frac{s}{t}\right)^2 + \tilde{C}\right]$$

$$iS_{\rm div}(p) = -\frac{1}{\epsilon^2}\frac{1}{2\pi}\sqrt{\frac{\lambda\mu^{2\epsilon}}{(-p)^\epsilon}} - \frac{1}{\epsilon}\frac{1}{4\pi}(1-\log 2)\sqrt{\frac{\lambda\mu^{2\epsilon}}{(-p)^\epsilon}}\,, \qquad (p=s,t)\,, \quad (20)$$

where $\tilde{C}$ is a constant. Here λ is the 't Hooft coupling defined by $\sqrt{\lambda} \equiv \sqrt{g^2_{\rm YM}N_c} = R^2/\alpha'$, and we have adopted units where $\alpha' = 1$. Dimensional regularisation has been employed in order to obtain a finite result for the area of the minimal surface, by going to $D = 4-2\epsilon$ dimensions (with $\epsilon < 0$).

This requires the introduction of an IR cutoff scale μ, having dimensions of mass, to account for the mass dimension of the D-dimensional coupling. In (20), we have separated a finite contribution from the divergent ones $iS_{\rm div}(p), (p = s, t)$, where the Mandelstam variables are defined here by

$$\begin{aligned} -s &= (k_1 + k_2)^2 = 2k_{1\mu}k_2{}^{\mu}\,, \qquad -t = (k_1 + k_4)^2 = 2k_{1\mu}k_4{}^{\mu}\,, \\ -u &= (k_1 + k_3)^2 = 2k_{1\mu}k_3{}^{\mu} = s + t\,. \end{aligned} \tag{21}$$

Note that the physical scattering region that we are considering here is $s, t < 0$ and $u > 0$, which is called the "u-channel" in the literature. Moreover, in the high-energy region one has $u \gg 1$ and t fixed, so that $-s \sim u$.

Now let us show that the two-gluon amplitude (20) is of the generic Regge form (1) with only one dominant Regge trajectory, namely of the form $A(s,t) \equiv (\frac{s}{s_0})^{\alpha(t)}\beta(t)$.

In order to display the Regge behaviour of the amplitude (20), it is convenient to expand the divergent contributions with respect to ϵ. One then obtains

$$\begin{aligned} iS_{\rm div}(p) &= -\frac{1}{\epsilon^2}\frac{\sqrt{\lambda}}{2\pi} + \frac{1}{\epsilon}\frac{\sqrt{\lambda}}{4\pi}\left(\log\frac{-p}{\mu^2} - 1 + \log 2\right) \\ &\quad -\frac{f(\lambda)}{16}\left(\log\frac{-p}{\mu^2}\right)^2 + \frac{g(\lambda)}{8}\log\frac{-p}{\mu^2} + \mathcal{O}(\epsilon)\,, \end{aligned} \tag{22}$$

where we have denoted

$$f(\lambda) = \frac{\sqrt{\lambda}}{\pi}\,, \qquad g(\lambda) = \frac{\sqrt{\lambda}}{\pi}(1 - \log 2)\,. \tag{23}$$

The meaning of $f(\lambda)$ and $g(\lambda)$ becomes clear if we rewrite Eq. (22) in terms of a new IR cutoff m, defined as (since ϵ is negative, $\epsilon \to 0_-$ corresponds to $m/\mu \to 0$, *i.e.*, to an infrared cutoff)

$$\frac{1}{\epsilon} \equiv \log\frac{m}{\mu}\,. \tag{24}$$

Neglecting terms which do not depend on p, we obtain

$$iS_{\rm div}(p) = -\frac{f(\lambda)}{16}\left(\log\frac{-p}{m^2}\right)^2 + \frac{g(\lambda)}{8}\log\frac{-p}{m^2} + (p\text{-independent terms})\,, \tag{25}$$

with $f(\lambda)$ appearing in front of the leading IR-divergent term proportional to $(\log m)^2$, and $g(\lambda)$ appearing in front of the sub-leading $(\log m)$ divergence.

It is important to note that $f(\lambda)$ appears (see, *e.g.*, Ref. [9] and references therein) in the expression of the cusp anomalous dimension $\Gamma_{\rm cusp}(\gamma)$, which represents the contribution of a cusp of boost parameter γ to the vacuum

expectation value of a Wilson loop in the fundamental representation. For large $|\gamma|$, one has indeed $\Gamma_{\rm cusp}(\gamma) \simeq -\big(f(\lambda)/4\big)|\gamma|$. The cusp anomalous dimension is relevant also for the calculation of the anomalous dimension γ_S of twist-two operators of large spin S, $\gamma_S \simeq f(\lambda)\log S$.

Using the expansion (22) and the definitions (23) and (24), the expression of the amplitude (20) simplifies to

$$\begin{aligned} \mathcal{A}^{\rm gluon}(s,t) &= C_\epsilon \left(\frac{-s}{m^2}\right)^{-\frac{f(\lambda)}{4}\log\frac{-t}{m^2}+\frac{g(\lambda)}{4}} \left(\frac{-t}{m^2}\right)^{\frac{g(\lambda)}{4}}, \\ C_\epsilon &= \exp\left(-\frac{\sqrt{\lambda}}{\pi}\frac{1}{\epsilon^2}+\tilde{C}+\mathcal{O}(\epsilon)\right). \end{aligned} \tag{26}$$

We note that the terms $\log(-s/\mu)^2$ and $\log(-t/\mu)^2$ in the finite part of Eq. (20) are compensated by corresponding terms of order ϵ^0 coming from the expansion (22) of $S_{\rm div}$ [10].

It is important to realize that formula (26) has precisely the form (1) of a dominant Regge amplitude with one contribution. Indeed, including for completeness also the Born term factor, which for large $-s$ and fixed t reads

$$\mathcal{A}_{\rm tree} \propto \frac{-s}{-t}, \tag{27}$$

the gluon–gluon scattering amplitude is of the form

$$\mathcal{A}(s,t) = \mathcal{A}_{\rm tree}\,\mathcal{A}^{\rm gluon}(s,t) = \beta(t)\left(\frac{-s}{m^2}\right)^{\alpha(t)}, \tag{28}$$

where $\alpha(t)$ is the *Regge trajectory*,

$$\alpha(t) = \alpha_0 + \alpha_1(t), \qquad \alpha_1(t) = -\frac{f(\lambda)}{4}\log\frac{-t}{m^2}, \qquad \alpha_0 = \frac{g(\lambda)}{4}+1, \tag{29}$$

and where $\beta(t)$ is given by

$$\beta(t) \propto C_\epsilon \left(\frac{-t}{m^2}\right)^{\frac{g(\lambda)}{4}-1} \tag{30}$$

up to a t-independent constant.

Following the Regge literature, the expression (29) is the result of the AdS/CFT calculation for the "Pomeron" Regge trajectory. In other terms, it corresponds to the dominant contribution to elastic scattering in the forward region for $\mathcal{N}=4$ SYM theory. The key property expected for a Regge trajectory is to be "universal", *i.e.*, present in all high-energy channels at

fixed momentum transfer for the same vacuum exchange quantum numbers. This leads us to compare the results obtained in the previous section with the eikonal method for two-quark scattering to those for gluon–gluon scattering discussed above, especially the Regge trajectory (29).

1.4. Two-quark versus two-gluon Regge amplitudes

For further comparison between the two-quark amplitude in the eikonal approach and the two-gluon Regge amplitude, we derive now the impact-parameter representation in both cases.

1.4.1. Two-quark impact-parameter amplitude

Let us go back to the resulting two-quark "amplitude" from the eikonal approach in its Euclidean formulation (18). In order to obtain the physical impact-parameter amplitude, one has to perform the analytic continuation from Euclidean to Minkowski space. Neglecting sub-leading contributions, and considering for definiteness the quark–quark s-channel (we are working with $A^{\text{quark}}_{\text{min}}(\pi-\theta,b,T)$), so that the relevant analytic continuation reads

$$\theta \to \pi + i\chi\,, \qquad T \to iT\,, \tag{31}$$

with $\chi \sim \log(s/M^2)$, $s>0$, we obtain

$$\begin{aligned} A^{\text{quark},\,s}_{\text{min,\,M}}(\chi,b,T) &= 2\Gamma_{\text{cusp}}(\chi)\log\frac{\Lambda b}{T\chi e^{i\pi}\left(1+e^{-i\frac{\pi}{2}}(\pi/\chi)\right)} \\ &= 2\Gamma_{\text{cusp}}(\chi)\log\frac{b}{T\chi}+\hat{\Psi}^s_{\text{M}}(\chi)\,, \end{aligned} \tag{32}$$

where we have used $\Gamma^{\text{E}}_{\text{cusp}}(\pi+i\chi)=\Gamma_{\text{cusp}}(\chi)$ [9]. Note that we used the superscript s in the notations in order to specify the physical channel $s\gg 0$ that we consider in Minkowski space. Taking the limit $\chi\to\infty$, we obtain for the b,T-dependent term and for the leading χ-dependence

$$A^{\text{quark},\,s}_{\text{min,\,M}}(\chi,b,T) = -\frac{f(\lambda)}{2}\chi\log\frac{b}{T\chi}+\mathcal{O}(\chi)\,, \tag{33}$$

where we have used the property [9] of the cusp anomalous dimension

$$\Gamma_{\text{cusp}}(\chi)\to -\frac{f(\lambda)}{4}\chi = -\frac{\sqrt{\lambda}}{4\pi}\chi \quad \text{for } \chi\gg 1 \tag{34}$$

which also implies that the auxiliary function $\hat{\Psi}^s_{\text{M}}(\chi)=\mathcal{O}(\chi)$ in (33).

The u-channel quark–quark amplitude,

$$\tilde{\mathcal{A}}^{\text{quark}}(\chi, b, T) \equiv \exp\left[-A^{\text{quark},\,u}_{\text{min, M}}(\chi, b, T)\right] \quad \left(= \imath\mathcal{A}^{\text{III}\bar{\text{I}}}(\chi, \lfloor, \mathcal{T})\right), \tag{35}$$

that we shall use for the comparison with the two-gluon scattering amplitude, is obtained by means of the crossing-symmetry relations

$$\theta \to -i\chi\,, \qquad T \to iT\,, \tag{36}$$

with $\chi \sim \log(-s/M^2)$, $u \sim -s > 0$, which yields

$$A^{\text{quark},\,u}_{\text{min, M}}(\chi, b, T) = 2\Gamma_{\text{cusp}}(i\pi - \chi)\log\frac{\Lambda b}{T\chi} = 2\Gamma_{\text{cusp}}(i\pi - \chi)\log\frac{b}{T\chi} + \mathcal{O}(\chi)\,. \tag{37}$$

Although the exact value of $\Gamma_{\text{cusp}}(i\pi - \chi)$ is not yet known, we expect that its large-χ behaviour coincides with that of $\Gamma_{\text{cusp}}(\chi)$ (this is actually the case in perturbation theory), so that in the limit $\chi \to \infty$ the leading term reads

$$A^{\text{quark},\,u}_{\text{min, M}}(\chi, b, T) = -\frac{f(\lambda)}{2}\chi\log\frac{b}{T\chi} + \mathcal{O}(\chi) \tag{38}$$

which also implies that a similar auxiliary function in the u-channel verifies $\hat{\Psi}^u_{\text{M}} = \mathcal{O}(\chi)$. Here, we note that the Regge limit of the quark–quark scattering amplitude has been evaluated also in Ref. [11] with techniques analogous to [8], and that the leading behaviour obtained for the amplitude agrees with the result of the eikonal method.

1.4.2. Two-gluon impact-parameter amplitude

The impact-parameter amplitude $\tilde{\mathcal{A}}^{\text{gluon}}(\hat{\chi}, b)$ is obtained by performing the two-dimensional Fourier transform of the amplitude $\mathcal{A}(s,t)$ with respect to the transverse momentum. Setting $-t = k^2$ with k the modulus of the transverse momentum, and including the usual factor s^{-1} in the definition of the impact-parameter amplitude, we obtain at large $-s$ (up to an irrelevant constant)

$$\tilde{\mathcal{A}}^{\text{gluon}}(\hat{\chi}, b) = C_\epsilon \int \frac{dk}{k}\, J_0(kb)\mathcal{A}^{\text{gluon}}\left(s, t = -k^2\right)\,, \tag{39}$$

where the hyperbolic angle $\hat{\chi}$ is defined as

$$\hat{\chi} = \log\frac{-s}{m^2} \tag{40}$$

as appropriate for a u-channel process.

Inserting the amplitude (20) into Eq. (39), one obtains

$$\begin{aligned}\tilde{\mathcal{A}}^{\text{gluon}}(\hat{\chi},b) &= C_\epsilon \left(m^2b^2\right)^{-\frac{1}{4}h(\hat{\chi};\lambda)} e^{\frac{g(\lambda)}{4}\hat{\chi}} K(\hat{\chi}) \,, \\ h(\hat{\chi};\lambda) &\equiv -f(\lambda)\hat{\chi} + g(\lambda) \,, \end{aligned} \tag{41}$$

where

$$\begin{aligned} K(\hat{\chi}) &\equiv \int_0^\infty d\zeta\, \zeta^{\frac{1}{2}h(\hat{\chi};\lambda)-1} J_0(\zeta) = 2^{\frac{h}{2}-1} \frac{\Gamma\left(\frac{h}{4}\right)}{\Gamma\left(1-\frac{h}{4}\right)} \\ &\approx \exp -\frac{f(\lambda)}{2}\hat{\chi}\left(\log\hat{\chi} + \log\frac{f(\lambda)}{2e} - i\frac{\pi}{2}\right) + \left(\frac{g(\lambda)}{2}-1\right)\log\hat{\chi} + \cdots \,, \end{aligned} \tag{42}$$

where we made use of a suitable analytic continuation (see [6] for all necessary details) in the physical Minkowski region where $\hat{\chi} \gg 1$, that is, $h \ll 0$ using the Stirling's formula, $\Gamma(z) \sim \sqrt{2\pi} e^{-z} z^{z-\frac{1}{2}}$ (for $|z| \to \infty$).

Taking into account the expansion (42), the resulting impact-parameter amplitude (41) can then be rewritten at high energy and in log form as the expansion

$$\begin{aligned} -\log\tilde{\mathcal{A}}^{\text{gluon}}(\hat{\chi},b) &= -\frac{f(\lambda)}{2}\hat{\chi}\log mb + \frac{f(\lambda)}{2}\hat{\chi}\log\hat{\chi} \\ &\quad + \hat{\chi}\left[\frac{f(\lambda)}{2}\left(\log\frac{f(\lambda)}{2e} - i\frac{\pi}{2}\right) - \frac{g(\lambda)}{4}\right] \\ &\quad + \log\hat{\chi}\left(1-\frac{g(\lambda)}{2}\right) + \frac{g(\lambda)}{2}\log mb + \cdots \,, \end{aligned} \tag{43}$$

1.4.3. Two-quark versus two-gluon impact-parameter Regge amplitudes

Let us finally compare our result (38) for quark–quark scattering, obtained in the eikonal approach, with (43) obtained for gluon–gluon scattering. For convenience, we rewrite here the u-channel quark–quark scattering amplitude,

$$\begin{aligned} -\log\tilde{\mathcal{A}}^{\text{quark}}(\chi,b,T) &= -\frac{f(\lambda)}{2}\chi\log\frac{b}{T\chi} + \mathcal{O}(\chi) \\ &= -\frac{f(\lambda)}{2}\hat{\chi}\log\frac{b}{T\hat{\chi}} + \mathcal{O}(\hat{\chi}) \,, \end{aligned} \tag{44}$$

where we used $\chi = \hat{\chi} + \log(m^2/M^2)$, compare with (40).

Examining the expression for the quark amplitude (44) following the order in the expansion of the exact expression (43) for the gluon one, the following consequences can be drawn:

- *First term*
  The first term exactly coincides with the leading term obtained in the case of two-gluon scattering, up to a rescaling $T \to m^{-1}$, *i.e.* up to a shift
  $$-\frac{f(\lambda)}{2}\hat{\chi}\log mT = \mathcal{O}(\hat{\chi})$$
  which plays a role at next to leading order only. Looking back to the discussion of the exact gluon–gluon amplitude (26), we noticed that the first term in its impact-parameter representation Eq. (43), coinciding with the leading term in (43) at high energy, was rooted at the origin of the Regge nature of the amplitude, and of the t-dependent part of the Regge trajectory (29). This implies that the quark–quark (and also quark–antiquark) scattering amplitude is of Regge type, and that the t-dependent part of the Regge trajectory is indeed the same obtained for gluon–gluon scattering.

  Hence the main conclusion is that the same Regge factor $(-s)^{-(f(\lambda)/4)\log(-t)}$ appears in the (s,t)-representation of both amplitudes. This corresponds to the fact that both amplitudes in impact-parameter space contain the same term, $2\Gamma_{\text{cusp}}(\hat{\chi})\log[(\text{mass})\,b/\hat{\chi}]$. This result is in agreement with the expected universality of the Regge trajectory, which should be independent of the colliding particles to which it is coupled. This is, therefore, a robust result, independent of the approximations we have performed.

  It is also interesting to note that the leading term of the order of $\hat{\chi}\log\hat{\chi}$ in the factorised $\hat{\chi}$-dependent part appears to be the same, while coming from seemingly different origin in the two cases: in the quark amplitude it comes from a refined evaluation of the cusp contribution, see *e.g.* (19), with the "generalised helicoid" ansatz, while in the gluon case it comes from the Fourier transform factor (42) after analytic continuation. As we have already remarked, this term is essential in order to obtain an amplitude of Regge type.

- *Second term*
  The $\mathcal{O}(\hat{\chi})$ term in (44) is compatible with the explicit expansion of the gluon amplitude. At the present stage we are not able to find a precise evaluation of this term, which could be obtained from the full solution of the minimal surface problem. However, as it has already been shown for the gluon case (see Eqs. (28)–(30)), it depends on the regularisation scheme. In particular, a t-dependent factorised term of the amplitude is not expected to be universal, but to depend on the spices of scattering particles.

An interesting while non-trivial question arises from the term $(f(\lambda)/2)\log f(\lambda)$ in (43) which does not seem to appear naturally in the quark amplitude (even if it only affects the $\mathcal{O}(\hat{\chi})$ term). Indeed, this $f \log f$ term cannot easily appear as a compensating term in the minimal surface calculation.

2. Reggeon exchange from Gauge/Gravity Duality

2.1. Introduction: Wilson loops, minimal surfaces and Gauge/Gravity duality for confining theories

Using the holographic AdS/CFT correspondence for the scattering amplitude in the eikonal approach we have confirmed that high-energy two-body amplitudes in $\mathcal{N} = 4$ SYM theory at strong coupling possess a Regge form with a *logarithmic* Regge trajectory. This is known not to be the case for the phenomenology of strong interaction two-body amplitudes, where the Regge behaviour is indeed satisfied but with *linear* Regge trajectories. From the theoretical point-of-view of the microscopic theory, *i.e.* Quantum Chromodynamics (QCD) one does not yet know how to derive the Regge behaviour at strong coupling and eventually test the linearity of the Regge trajectories. In papers [4, 5], the authors have given a first hint on this problem by considering the Gauge/Gravity duality for a generic confining, and thus non-conformal, case.

In order to extend the duality to the confining case, one has to properly modify the background metric in the dual gravity theory, taking into account that the theory is no more conformal. Although the precise realisation of the duality (assuming it exists) is not known yet, a common feature of various attempts to describe a confining theory in terms of a gravity dual is the presence of a characteristic scale R_0 in the metric, which separates the small and large z regions. With the appropriate choice of coordinates, while for small z the metric diverges as some inverse power of z, for z of the order of R_0 it turns out to be effectively flat. The interpretation in the dual confining field theory is that the scale R_0 provides the confinement scale. For example, in the case of the AdS/BH metric of [12], such a scale is provided by the position in the fifth dimension of the black–hole horizon. The relevant part of the metric reads

$$ds^2_{\mathrm{AdS/BH}} = \frac{16}{9}\frac{1}{f(z)}\frac{dz^2}{z^2} + \frac{\eta_{\mu\nu}dx^\mu dx^\nu}{z^2} + \dots , \tag{45}$$

where $f(z) = z^{2/3}(1 - (z/R_0)^4)$.

The starting point of [4,5] was to remark that the near-horizon geometry

is effectively flat

$$ds^2_{\rm hor} \simeq \frac{1}{R_0^2}\eta_{\mu\nu}dx^\mu dx^\nu \,. \tag{46}$$

This allowed to make the approximation of reducing the minimal surface problem to flat space, and thus to consider the proper *helicoid geometry* which was introduced in the beginning of Section 1, and for which an analytic approach is possible. In paper [4], the elastic "Pomeron" amplitude has been studied while in [5], the inelastic "Reggeon" one was discussed. In both cases, a Regge form with *linear* trajectories were found. In the following, we shall discuss in more detail the Reggeon case (with some consequence for the Pomeron), which were thoroughly reanalysed recently in [13] which will now present and put in perspective with the conformal case.

Let us recall the method of Ref. [5] for the determination of the Reggeon-exchange contribution to the meson–meson scattering amplitude in the *soft* high-energy regime. The starting point is to adopt a description of the interacting hadrons in terms of their constituent partons. Such an approach to *soft* high energy hadron–hadron scattering has been introduced in [14], where it was used, together with an LSZ reduction scheme and an eikonal approximation for the propagators, in order to derive approximate non-perturbative formulas for the scattering amplitudes. The basic idea is that the leading Pomeron-exchange contribution to the elastic amplitude comes from processes which are elastic and *soft* at the level of the constituent partons, justifying an eikonal-like approach. In a space-time picture of these processes, the partons travel along their classical, straight-line trajectories, exchanging only *soft* gluons which leave these trajectories practically unperturbed.

In particular, in the case of meson–meson scattering, one can describe the mesons, in a first approximation, in terms of a wave packet of transverse colourless quark–antiquark dipoles. The mesonic scattering amplitude is reconstructed, after folding with the appropriate wave functions, from the scattering amplitude of such dipoles. Since here we are interested only in the Reggeon trajectory, which, being a universal quantity, should not depend on the details of the meson wave function, we can focus on the dipole–dipole amplitude, which is expected to encode the relevant features of the process. Stated differently, invoking the universality of Reggeon exchange, one can consider mesons whose wave function is strongly peaked around some average value $|\vec{R}|$ of the dipole size.

Using this simplified description for the mesons, Reggeon exchange is identified as an inelastic process at the partonic level, involving the exchange of a quark–antiquark pair between the colliding dipoles. More precisely, the corresponding space-time picture is the following (see Fig. 8). Before and after the interaction time (which may be long for a *soft* interaction), the partons inside the high-energy mesons travel approximately along their

classical, straight-line (*eikonal*) trajectories. During the interaction time, a pair of valence partons is exchanged in the t channel between the mesons, and thus their trajectories bend, connecting the incoming and outgoing eikonal trajectories; the other partons exchange only *soft* gluons, and their straight-line trajectories are left practically undisturbed. The softness of the process requires that the exchanged fermions carry a small fraction of longitudinal momentum of the mesons.

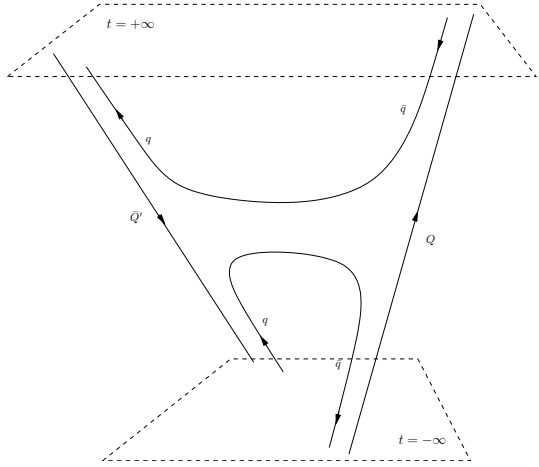

Fig. 8. Space-time picture of the Reggeon-exchange process. Q, $\bar{Q}'$ are heavy and fast quark and antiquark, which follow straight-line trajectories in the eikonal approximation. q, $\bar{q}$ are the exchanged light quark and antiquark, describing the Reggeon exchange between the incident $Q\bar{q}$ and $\bar{Q}'q$ mesons (see text).

In order to avoid inessential complications, we consider the scattering of two heavy-light mesons $M_{1,2}$ of large mass $m_{1,2}$, *i.e.*, $M_1 = Q\bar{q}$ and $M_2 = \bar{Q}'q$, where Q and $\bar{Q}'$ are heavy and of different flavours, while q and $\bar{q}$ are light and of the same flavour. In this way the total scattering amplitude amounts to a single type of Reggeon-exchange process, namely the one in which q and $\bar{q}$ are exchanged in the t channel, plus the Pomeron-exchange component, where there are no exchanged fermions. Moreover, the choice of heavy mesons is made in order for the typical size of the dipoles to be small, since in this case $|\vec{R}_{1,2}| \sim m_{1,2}^{-1} \ll \Lambda_{\rm QCD}^{-1}$; the reasons for this choice will be explained later on.

At this point, let us describe the expression for the Reggeon-exchange contribution $\mathcal{A}_{\mathcal{R}}(s,t)$ to the scattering amplitude proposed in [5]. To this extent, let us introduce the impact-parameter amplitude $a(\vec{b},\chi)$,

$$\mathcal{A}_{\mathcal{R}}(s,t) = -i2s \int d^2b \; e^{i\vec{q}\cdot\vec{b}} a\left(\vec{b},\chi\right) , \tag{47}$$

where χ is the hyperbolic angle between the classical trajectories of the colliding mesons, related to the center-of-mass energy squared s through $\chi \simeq \log s/(m_1 m_2)$ (for $s \to \infty$), with $m_{1,2}$ the masses of the mesons, and $t = -\vec{q}^{\,2}$. According to the space-time picture of the process given above, the eikonal approximation can no longer be used to describe the propagation of the light quarks. Working in Euclidean space, the authors of [5] exploit the path-integral representation for the fermion propagator in an external non-Abelian gauge field, in order to write down a Euclidean "amplitude" $\tilde{a}(\vec{b}, \theta, T)$ in terms of a path-integral over the trajectories of the light quarks. Here θ is the angle between the Euclidean trajectories of the mesons, and T is the IR cutoff.

All in all, as discussed in detail in [13], the Euclidean "amplitude" $\tilde{a}(\vec{b}, \theta, T)$, which should encode the features of the Reggeon trajectory, can be written symbolically as

$$\tilde{a}\left(\vec{b}, \theta, T\right) = \mathcal{Z}^{-1} \int \mathcal{D}\mathcal{C}_+ \mathcal{D}\mathcal{C}_- \, \langle \mathcal{W}[\mathcal{C}] \rangle \, e^{-m_0 L[\mathcal{C}]} \, \mathcal{I}[\mathcal{C}] \,, \tag{48}$$

where the different terms $\langle \mathcal{W}[\mathcal{C}] \rangle, L[\mathcal{C}], \mathcal{I}[\mathcal{C}], \mathcal{Z}$ are defined as follows:

- $\langle \mathcal{W}[\mathcal{C}] \rangle$ is the expectation value of the Euclidean Wilson loop running along the path $\mathcal{C}$ (see Fig. 9), composed essentially of the Euclidean trajectories of the partons. More precisely, $\mathcal{C}_1$ and $\mathcal{C}_2$ are the straight-line paths corresponding to the heavy partons Q and $\bar{Q}'$, respectively, which are fixed following the eikonal approximation framework. $\mathcal{C}_{+,-}$ are the curved paths corresponding to the exchanged light partons, which have to be integrated over. Finally, $\mathcal{S}^{\pm}_{1,2}$ are straight-line paths in the transverse plane (see Fig. 9), connecting the four pieces above. The path-integration over the exchanged-quark trajectories $\mathcal{C}_\pm$ is denoted symbolically by $\int \mathcal{D}\mathcal{C}_\pm$.
- $L[\mathcal{C}]$ is the length of the path travelled by the light quarks,

$$L[\mathcal{C}] \equiv L[\mathcal{C}_+] + L[\mathcal{C}_-] = L_+ + L_- \,, \tag{49}$$

  and m_0 is the (bare) mass of the light quark. As we will see below in more detail, the length-term factor $e^{-m_0 L[\mathcal{C}]}$ in Eq. (48) plays an important stabilisation role in the minimisation procedure related to the saddle-point approximation of the path-integral.
- $\mathcal{I}[\mathcal{C}] \equiv \otimes_{i=\{1,2,+,-\}} \mathcal{I}_i[\mathcal{C}_i]$ is the product of the spin factors corresponding to the various fermionic trajectories, and it comes from the integration over momenta in the path-integral representation for the fermion propagator.

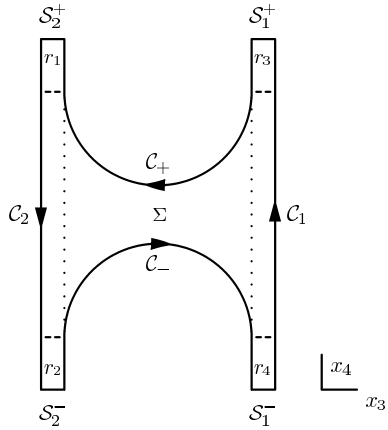

Fig. 9. Schematic representation of the Wilson loop contour relevant to Reggeon exchange. The "tilted" contour (solid line) is projected on the $(x_4 - x_3)$ plane for simplicity. The dashed lines delimit the various regions of the corresponding minimal surface, to be discussed below. The dotted lines correspond to the "virtual" eikonal trajectories of the light quarks, which together with $\mathcal{C}_{1,2}$ describe the free propagation of the mesons.

- $\mathcal{Z}$ is a normalisation constant whose role is to make the amplitude IR-finite. In principle, one should be able to determine it from first principles; at the present stage, we adopt a more pragmatic approach, fixing it "by hand" in order to remove infrared divergences.

2.2. The Euclidean holographic problem: the "twisted soap film"

The following step is the application of the gauge/gravity correspondence, which, as written in (2), allows to write the Wilson-loop expectation value as

$$\langle \mathcal{W}[\mathcal{C}] \rangle = \mathcal{F}[\mathcal{C}]\ e^{-\frac{1}{2\pi\alpha'_{\text{eff}}} A_{\min}[\mathcal{C}]}, \tag{50}$$

where $A_{\min}[\mathcal{C}]$ is the area of the minimal surface having the contour $\mathcal{C}$ as boundary, and $\mathcal{F}[\mathcal{C}]$ contains the contributions of fluctuations around this surface.

At this point, one should in principle solve the Plateau problem in a curved background for a general boundary, and then integrate over all possible boundaries: this is a formidable task, which is currently out of reach. In order to simplify the problem, it is useful to recall the physical picture of the process, already discussed above, and sketched in Fig. 8. Before and after the interaction, the partons travel along their eikonal, straight-line trajectories, and during the time of interaction the light quarks are exchanged between the two mesons. Translating this picture to Euclidean space, we

then expect that the main contributions to the path integral come from those paths $\mathcal{C}_\pm$ which away from the central (interaction) region are straight lines, coinciding with the eikonal trajectories of the light quarks. As a consequence, the relevant minimal surfaces are essentially made up of a central strip (corresponding to region Σ in Fig. 9), bounded by the curved part of the light-quark trajectories, which corresponds to the exchanged Reggeon, and four rectangles (regions $r_{1,2,3,4}$ in Fig. 9), corresponding to the free propagation of mesons before and after the interaction.

In the central region, the minimal surface is expected to be made up of an almost vertical wall of area $A_{\rm wall}$, extending from the boundary of AdS up to the region where the metric is effectively flat (*e.g.*, the black-hole horizon of Ref. [12]), and a minimal surface living in the effectively flat metric, bounded by the light-quark trajectories transported from the boundary of AdS to the effectively flat region, see Fig. 2 (left).

Within this configuration, the geometry of the flat part of the Reggeon strip is governed by the (almost) infinite straight lines corresponding to the eikonal trajectories of the heavy quarks, transported to the effectively flat region. This suggests that the relevant contributions come from configurations in which the floating boundaries lie on the corresponding *helicoid*. Indeed, the helicoid has been recognised as the minimal surface associated with *soft* elastic quark–quark (and also quark–antiquark) scattering at high energy [4]. This assumption is expected to be sensible only for small quark mass, as we will discuss further on. We then recover the same basic geometry already found in the treatment of Pomeron exchange, the difference being the presence of partially floating, instead of fully fixed boundaries.

To first order the flat part of the "strip" Σ takes the form

$$X^{\rm helicoid}(\bar\tau,\sigma) = \left(\cos\left(\frac{\theta\sigma}{b}\right)\bar\tau\,,\,\sin\left(\frac{\theta\sigma}{b}\right)\bar\tau\,,\,\frac{\vec b}{b}\,\sigma\right)\,, \qquad (51)$$
$$\sigma\in[-b/2,b/2]\,,\qquad \bar\tau\in\left[-\tau^-(\sigma),\tau^+(\sigma)\right]\,,\qquad \tau^\pm(\sigma)\geq 0\,.$$

The path-integral is then reduced to the integration over the curved part of the light-quark trajectories, constrained now to lie on the helicoid, *i.e.*, over the "profiles" $\tau^\pm(\sigma)$ which constitute the boundary of the relevant piece of helicoid; the remaining parts of the paths $\mathcal{C}_\pm$ lie on the eikonal light-quark trajectories. Notice that for any choice of $\tau(\sigma)$ in Eq. (51), the resulting surface is automatically a minimal surface in flat space, *i.e.*, a surface with zero mean curvature.

The remaining part of the minimal surface is made up of the vertical wall and of the four rectangles. In turn, the vertical wall is made of four pieces, corresponding to the paths $\mathcal{C}_\pm$ and to those pieces of the paths $\mathcal{C}_{1,2}$ bounding the interaction region (*i.e.*, between the dashed lines in Fig. 9). The

rectangles are deformed in the region where they connect to the interaction region (near the dashed lines in Fig. 9), where the surface rises steeply to the effectively flat region; nevertheless, the area of these regions is proportional to $|\vec{R}_{1,2}|$, and can be neglected.

After estimating, see [13] for all details, the various contributions to the functional integral (48) one uses a saddle-point approximation: exploiting the symmetry of the configuration in order to restrict to the case $\tau^+(\sigma) = \tau^-(\sigma) \equiv \tau(\sigma)$, one has to solve the Euler–Lagrange equations $\delta S_{\text{eff, E}}[\tau_{\text{s.p.}}(\sigma)] = 0$, to find the profile $\tau_{\text{s.p.}}(\sigma)$ which minimises the "effective action"

$$S_{\text{eff, E}}[\tau(\sigma)] \equiv \frac{1}{2\pi\alpha'_{\text{eff}}} A^{\text{hel}}_{\text{min}}[\tau(\sigma)] + 2m \left(L^{\text{hel}}[\tau(\sigma)] - L_0[\tau(\sigma)] \right) , \tag{52}$$

where the area $A^{\text{hel}}_{\text{min}}$ of the helicoidal "Reggeon strip", and the length L^{hel} of the boundaries, can be written explicitly as functionals of $\tau^{\pm}(\sigma)$, namely

$$A^{\text{hel}}_{\text{min}} \left[\tau^+, \tau^-\right] = \int_{-\frac{b}{2}}^{+\frac{b}{2}} d\sigma \int_{-\tau^-(\sigma)}^{+\tau^+(\sigma)} dx \, \sqrt{1 + (px)^2} \, ,$$

$$L^{\text{hel}} \left[\tau^{\pm}(\sigma)\right] = \int_{-\frac{b}{2}}^{+\frac{b}{2}} d\sigma \, \sqrt{1 + (p\tau^{\pm}(\sigma))^2 + (\dot{\tau}^{\pm}(\sigma))^2} \, , \tag{53}$$

using the notation

$$p = \theta / b \, , \tag{54}$$

with L_0 depending only on the endpoints

$$L_0 \left[\tau^{\pm}\right] = \tau^{\pm} (b/2) + \tau^{\pm} (-b/2) \, . \tag{55}$$

In the general case, the variational problem defined in Eq. (52) is aimed at the determination of an "optimal" boundary, involving in the minimisation procedure both the area of the resulting surface and the length of the boundary. This is what we call [13] *minimal surface problem with floating boundaries.*

2.2.1. Warm-up exercise: soap film with floating boundaries

Before attacking the minimisation problem relevant to Reggeon exchange in full generality, we want to discuss a simpler case, namely the case in which the straight lines forming the fixed part of the boundary are parallel,

i.e., $\theta = 0$. This configuration is of limited interest for our problem, since our purpose is to obtain an analytic dependence on θ; nevertheless, the mathematical problem is similar, and moreover in this case the variational equations can be solved explicitly, so that we can obtain a few indications in the study of the more complicated "tilted" case $\theta \neq 0$.

We consider then the minimisation of a functional simpler but similar to (52) namely

$$S_{\text{planar}}[\tau(\sigma)] = \frac{1}{2\pi\hat{\alpha}'} A[\mathcal{C}_1, \mathcal{C}_2] + \hat{m}\,(L[\mathcal{C}_1] + L[\mathcal{C}_2])\ , \tag{56}$$

where A is the area of a surface bounded on two opposite sides by two parallel straight lines of length $2T$ at a distance R, which are held fixed. On the other sides, the surface is bounded by two *a priori* free lines following the paths $\mathcal{C}_{1,2}$, of length $L[\mathcal{C}_{1,2}]$, which have to be determined by the minimisation procedure.

For want of a physical interpretation, this functional corresponds to the energy of an ideal soap film of vanishing mass and of surface tension $1/2\pi\hat{\alpha}'$, extending between two rigid rods (the straight lines) parallel to the ground, and between two flexible (massless) wires (of length larger than $2T$), each passing through two rings positioned at the endpoints of the rods (see Fig. 10); moreover, two equal masses M are attached at the endpoints of each wire, with $Mg = \hat{m}$, and their potential energy in the gravitational field contributes the length term.

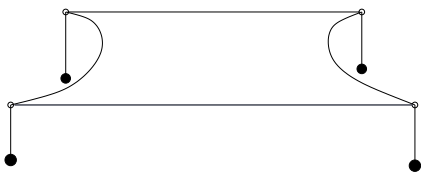

Fig. 10. Soap film with partially floating boundary. The straight lines correspond to rigid rods, the curved lines to flexible wires, attached to four equal masses (black balls).

Given the symmetries of the problem, the solution will be a planar surface, and the two floating boundaries will be one the reflection of the other. The problem is thus effectively two-dimensional, and we can parameterise the relevant surfaces in terms of a single function $\tau(\sigma)$, *i.e.*

$$\begin{aligned} &X^{\text{plan}}[\tau(\sigma); \bar{\tau}, \sigma] = (\bar{\tau}, \sigma)\,, \qquad && \sigma \in [-R/2, R/2]\,, \\ &\bar{\tau} \in [-\tau(\sigma), \tau(\sigma)]\,, && \tau(\sigma) > 0\,. \end{aligned} \tag{57}$$

The expression of the functionals simplifies therefore to

$$L = \int_{-\frac{R}{2}}^{+\frac{R}{2}} d\sigma \sqrt{1 + (\dot{\tau}(\sigma))^2}\,, \qquad A = 2 \int_{-\frac{R}{2}}^{+\frac{R}{2}} d\sigma\ \tau(\sigma)\,. \tag{58}$$

Notice that τ must satisfy $\tau(\sigma) = \tau(-\sigma)$ because of the symmetries of the problem. The Euler–Lagrange equation is easily derived, and reads

$$\ddot{\tau} - 2R_{\rm c}^{-1}\left(1 + \dot{\tau}^2\right)^{\frac{3}{2}} = 0\,, \tag{59}$$

where the combined parameter

$$R_{\rm c} \equiv 4\pi\hat{\alpha}'\hat{m}\,, \tag{60}$$

will play an important role as a critical value for R in the minimisation problem. Notice that for $R_{\rm c} > 0$ we have $\ddot{\tau} > 0$. This equation reflects the general expectation on the nature of the two terms contributing to the energy functional, discussed in the previous section. For large $R_{\rm c}$ the first "length" term in (59) dominates, so that the equation reduces to that of a straight line; the second "area" term increases the curvature of the free boundary, bending it inwards.

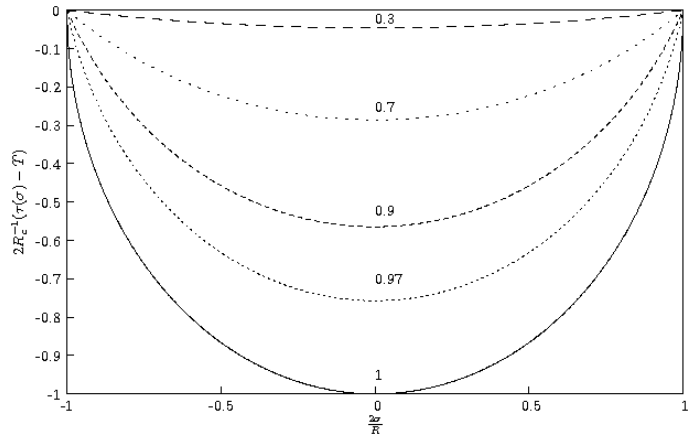

Fig. 11. Minimisation profile of the floating boundary. Half of the floating boundary is represented after minimisation for various values of $R/R_{\rm c}$. The opposite half of the floating boundary is obtained by reflection with respect to the horizontal axis.

This equation is solved in the standard way by setting (see *e.g.* [13])

and gives the solution

$$\tau(\sigma) - \tau_0 = \frac{R_c}{2}\left[1 - \sqrt{1 - \left(\frac{2\sigma}{R_c}\right)^2}\right], \tag{61}$$

with

$$\tau_{\min}(\sigma) = T - \frac{R_c}{2}\left[\sqrt{1 - \left(\frac{2\sigma}{R_c}\right)^2} - \sqrt{1 - \left(\frac{R}{R_c}\right)^2}\right]. \tag{62}$$

The minimisation profile of the floating boundary is depicted in Fig. 11. Notice that in order for $\tau(\sigma)$ to be real, we need the following condition to be satisfied:

$$R \leq R_c \equiv 4\pi\hat{\alpha}'\hat{m}\,. \tag{63}$$

The condition Eq. (63) simply means that when the bound is reached, the flexible wire runs parallel to the rigid rod at the junction point. Indeed, if R exceeds the critical value R_c at fixed $\hat{\alpha}$ and $\hat{m}$ (more precisely, at fixed $\hat{\alpha}\hat{m}$), or equivalently if R_c becomes smaller than R (*e.g.* for too large surface tension or too small mass), the force due to the surface tension is stronger than the gravitational force on the masses, and it makes the soap film collapse. This is essentially a Gross–Ooguri transition [15], which we expect to find also in the *tilted* helicoidal case $\theta \neq 0$, and R_c appears to be the corresponding critical value at which the transition takes place.

2.2.2. Tilted soap film with floating boundaries

In this section, we discuss the Euclidean variational problem relevant to the Reggeon-exchange amplitude, *i.e.*, for the "tilted" configuration of Fig. 8. The "effective action" functional Eq. (52) is rewritten here for convenience

$$S_{\text{eff, E}}[\tau(\sigma)] = \frac{1}{2\pi\alpha'_{\text{eff}}} A^{\text{hel}}_{\min}[\tau(\sigma)] + 2m\left(L^{\text{hel}}[\tau(\sigma)] - L_0[\tau(\sigma)]\right). \tag{64}$$

Our aim is to find a smooth "profile" $\tau(\sigma)$, bounding a piece of helicoid which connects two straight lines at a transverse distance b, and forming an angle θ in the longitudinal $(x_4 - x_1)$ plane, see Fig. 8. In order to do so, it is convenient to pass to dimensionless coordinates by making the change of variables

$$t(s) = p\tau(\sigma)\,, \qquad s = p\sigma\,, \qquad px = y \qquad \text{with} \qquad p = \theta/b\,. \tag{65}$$

Note that $\dot{t} \equiv \frac{dt}{ds} = \frac{d\tau}{d\sigma} = \dot{\tau}$. In terms of these reduced variables, the expressions for the area and length functionals Eq. (53) read

$$\begin{aligned} A^{\text{hel}}_{\text{min}} &= \frac{1}{p^2} \int\limits_{-\frac{\theta}{2}}^{+\frac{\theta}{2}} ds \int\limits_{-t(s)}^{+t(s)} dy \, \sqrt{1+y^2}\,, \\ L^{\text{hel}} &= \frac{1}{p} \int\limits_{-\frac{\theta}{2}}^{+\frac{\theta}{2}} ds \, \sqrt{1+[t(s)]^2+[\dot{t}(s)]^2}\,, \end{aligned} \tag{66}$$

and moreover

$$L_0 = \frac{1}{p}\Big[t\left(\tfrac{\theta}{2}\right) + t\left(-\tfrac{\theta}{2}\right)\Big] \tag{67}$$

for the subtraction term. This term will not enter the variational equations, since the value of $\tau(\pm\frac{b}{2})$, and so that of $t(\pm\frac{\theta}{2})$, is determined by requiring a smooth transition to the eikonal straight-line paths: in other words, we perform the variation of the effective action at $t(\pm\frac{\theta}{2})$ fixed, we solve the equation and we subsequently determine the value which makes the path smooth. In terms of our parameterisation, in order for the part of the path on the helicoid to be smoothly connected with the incoming and outgoing straight lines, we need that $\dot{t}(\pm\frac{\theta}{2}) = \pm\infty$.

It is straightforward to obtain the Euler–Lagrange equation corresponding to the minimisation of the functional, which reads explicitly

$$\frac{2m}{p}\frac{1}{\left(1+t^2+\dot{t}^2\right)^{\frac{3}{2}}}\left[\left(\ddot{t}-t\right)\left(1+t^2\right)-2t\dot{t}^2\right] - \frac{1}{\pi\alpha'_{\text{eff}}p^2}\sqrt{1+t^2} = 0\,. \tag{68}$$

After setting

$$t(s) = \frac{\theta}{b}\tau(\sigma) \equiv \sinh\varphi(s)\,, \qquad \lambda \equiv \frac{1}{2\pi\alpha'_{\text{eff}}mp} = \frac{b}{2\pi\alpha'_{\text{eff}}m\theta}\,, \tag{69}$$

the equation takes the simpler form

$$\ddot{\varphi} - \left(1+\dot{\varphi}^2\right)\tanh\varphi - \lambda\left(1+\dot{\varphi}^2\right)^{\frac{3}{2}}\cosh\varphi = 0\,. \tag{70}$$

In some sense, the variable φ parameterises in a scale-invariant way the development in "time" of the quark-exchange process in Euclidean space.

All in all, after a series of non-trivial transformations of the equations and boundary conditions to reach a formal solution (see [13] for all necessary

details of the proof), the final answer for the minimum Euclidean action reads

$$S_{\mathrm{eff,\,E}} = \frac{b^2}{2\pi\alpha'_{\mathrm{eff}}\theta}\, f\left(\tilde{\varphi}\right) + \frac{4mb}{\theta}\left(B(\varphi_0,\tilde{\varphi}) - \sinh\tilde{\varphi}\right), \tag{71}$$

where

$$B\left(\varphi_0,\tilde{\varphi}\right) = \int_{\varphi_0}^{\tilde{\varphi}} d\varphi \sqrt{(\cosh\varphi)^2 - \left[\frac{\lambda}{2}\left(f\left(\tilde{\varphi}\right) - f(\varphi)\right)\right]^2}, \tag{72}$$

$$\tau_0 \equiv \sinh\varphi(0)\,, \qquad \tau\left(\pm\frac{b}{2}\right) \equiv \sinh\tilde{\varphi}\,, \tag{73}$$

and the function

$$f(\varphi) = \varphi + \sinh\varphi\cosh\varphi\,. \tag{74}$$

The last term in Eq. (71) is simply the subtraction term $2mL_0$, rewritten in terms of $\tilde{\varphi}$. The other two terms are obtained by combining in Eq. (64) the expressions for the area of the piece of helicoid and the length of its curved boundaries. A sketch of the minimisation profile (along the helicoid sheet and projected on a plane) for the floating boundary is given in Fig. 12, together with the geometric meaning of the variables$\tau, \varphi, \tilde{\varphi}$.

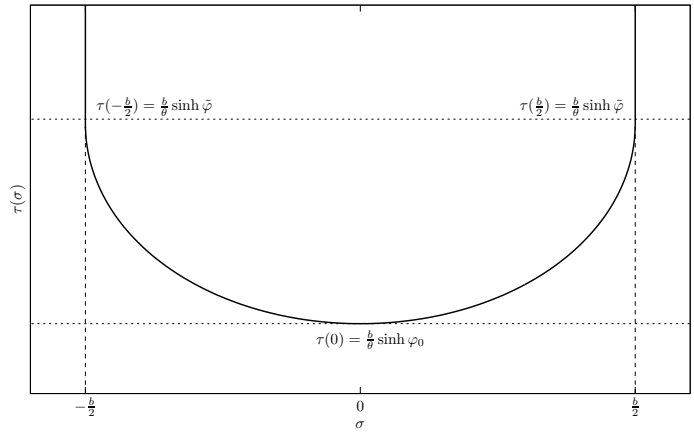

Fig. 12. Sketch of the minimisation profile $\tau(\sigma)$ described by the trajectories of the exchanged fermions on the helicoid. The solid line represents the trajectory of the exchanged fermion. The dashed (vertical) lines are the eikonal trajectories, plotted for reference. The dotted (horizontal) lines indicate the minimal and maximal values of $\tau(\sigma)$, *i.e.*, $\tau(0) = \frac{b}{\theta}\sinh\varphi_0$ and $\tau(\pm\frac{b}{2}) = \frac{b}{\theta}\sinh\tilde{\varphi}$.

It is possible to prove that a regular solution, for which $\tau(s) > 0$, and thus $\varphi(s) > 0$, can exist only in a limited range for the impact parameter.

From Eq. (70), using the fact that $\varphi(s) \geq \varphi_0$, we derive the inequality

$$\frac{\ddot{\varphi}}{(1+\dot{\varphi}^2)^{\frac{3}{2}}} \geq \lambda \cosh\varphi \geq \lambda \cosh\varphi_0 \tag{75}$$

which integrating between 0 and $\theta/2$, and using $\dot{\varphi}(0) = 0$ and $\dot{\varphi}(\theta/2) = \infty$, provides a bound on b

$$\frac{\lambda\theta}{2} = \frac{b}{4\pi\alpha'_{\text{eff}}m} \leq \frac{1}{\cosh\varphi_0} \leq 1\,. \tag{76}$$

This defines a *critical* value

$$b_{\text{c}} \equiv 4\pi\alpha'_{\text{eff}}m \tag{77}$$

beyond which the Euclidean solution ceases to be a positive real quantity.

The limitation imposed by this bound is analogous to the one found in the case $\theta = 0$, Eq. (63), *i.e.*, for too large b the four-dimensional Euclidean "soap film" corresponding to the string world-sheet collapses due to the attractive effect of the string tension. Moreover, the fact that b_{c} vanishes when $m = 0$ reflects the necessity of a "repulsive" boundary-length term to compensate for the "attractive" area term in the minimisation procedure.

For the moment, we have only a solution of the variational problem under an implicit and rather involved form. It is possible to obtain a reliable analytic approximation in the case $\lambda \gg 1$ useful for the further discussion where, recalling (69),

$$\lambda \equiv \frac{1}{2\pi\alpha'_{\text{eff}}mp} = \frac{b}{2\pi\alpha'_{\text{eff}}m\theta} = \frac{b}{b_{\text{c}}}\frac{2}{\theta}\,. \tag{78}$$

We determine now the explicit form of the solution in the large λ limit, which is expected to describe the small-θ Euclidean region, namely $\theta \ll b/(2\pi\alpha'_{\text{eff}}m) = 2b/b_{\text{c}} \leq 2$.

All calculations done [13], the whole system of equations boils down to

$$\cosh\tilde{\varphi} = \frac{4\pi\alpha'_{\text{eff}}m}{b} = \frac{b_{\text{c}}}{b}\,, \tag{79}$$

$$\tilde{\varphi} - \varphi_0 = \frac{\theta}{2}\,, \tag{80}$$

and thus

$$\varphi_0 = \tilde{\varphi} - \Delta = \operatorname{arccosh}\frac{b_{\text{c}}}{b} - \frac{\theta}{2}\,, \tag{81}$$

allowing to get an explicit expression of the floating boundary geometry, *i.e.* $(\varphi_0, \tilde{\varphi})$ in Fig. 13 in terms of the kinematic variables of the Euclidean eikonal configuration of the two-body reaction *i.e.* (b, θ).

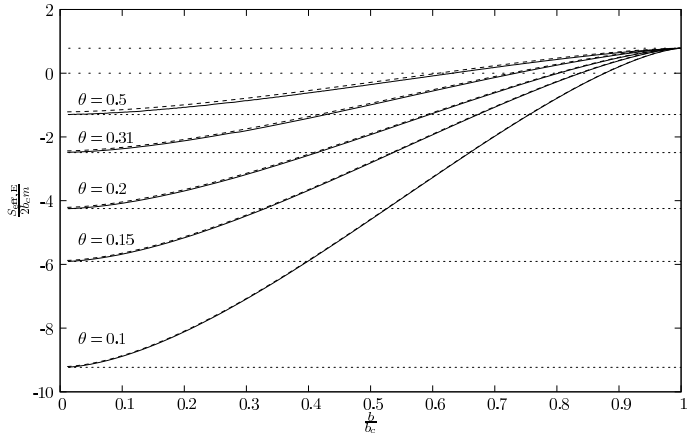

Fig. 13. Effective action as a function of b for various values of θ: small θ. The action is plotted in units of $2b_{\rm c}m = 8\pi\alpha'_{\rm eff}m^2$. The solid lines represent the numerical results for the exact solution and the dotted lines represent the analytical result obtained in the case $\varphi_0 \gg 1$. and the dashed lines represent the analytical result obtained in the case $\lambda \gg 1$.

It is now not too difficult to obtain the effective action (71), after we have computed the integral (72), namely

$$B\left(\varphi_0, \tilde{\varphi}\right) = \Delta \int_0^1 dx \sqrt{1-x^2}\left[\cosh\tilde{\varphi} + \mathcal{O}(\theta)\right] = \frac{\theta\pi}{8}\cosh\tilde{\varphi} + \mathcal{O}\left(\theta^2\right) . \quad (82)$$

Substituting $\tilde{\varphi} = \operatorname{arccosh}\frac{b_{\rm c}}{b}$ into the other two terms of (71) we finally obtain

$$S_{\rm eff,\,E}\big|_{\lambda\gg 1} = \frac{b^2}{2\pi\alpha'_{\rm eff}\theta}\operatorname{arccosh}\frac{b_{\rm c}}{b} + 2\pi^2\alpha'_{\rm eff}m^2 - \frac{2bm}{\theta}\sqrt{\left(\frac{b_{\rm c}}{b}\right)^2 - 1} \quad (83)$$

up to order $\mathcal{O}(\theta^0)$.

The usefulness of this approximation is that, even if restricted to small values of θ, it extends up to "large" values of b, *i.e.*, up to $b_{\rm c} = 4\pi\alpha'_{\rm eff}m$. This is clearly demonstrated in Fig. 13, where the approximation (83) is compared with the numerical evaluation coming from the exact solution.

As we will discuss in detail in the next section, the physically interesting region in Minkowski space lies at large impact-parameter values, and an appropriate extension in b beyond $b_{\rm c}$ will be required. Indeed, we see from Eq. (79) that in order to perform this extension, we have to analytically continue beyond the value $\tilde{\varphi} = \operatorname{arccosh}\frac{b_{\rm c}}{b} = 0$ *i.e.* $\frac{b_{\rm c}}{b} = 1$.

2.3. From Euclid to Minkowski: the holographic Reggeon amplitude

A real solution of the saddle-point equation in Euclidean space exists only in a limited range of impact-parameter values. The limitation to real solutions is dictated by the fact that the path-integral Eq. (48) is over real paths $\mathcal{C}_\pm$ in Euclidean space, leading in turn to an integral over real $\tau^\pm$. The limitation $b \leq b_c$ can be seen also in the effective action (83), since b_c is a branch point for this quantity, beyond which it acquires an imaginary component. Indeed, making then the substitution $\theta \to -i\chi$ in Eq. (83), we obtain

$$S_{\text{eff, E}}|_{\lambda \gg 1} \to S_{\text{eff, M}} = i\frac{b^2}{2\pi\alpha'_{\text{eff}}\chi}\operatorname{arccosh}\frac{b_c}{b} - i\frac{2bm}{\chi}\sqrt{\left(\frac{b_c}{b}\right)^2 - 1} + 2\pi^2\alpha'_{\text{eff}}m^2\,. \tag{84}$$

The real part of expression Eq. (84) consists simply of a b, χ-independent term, while the whole b, χ-dependence is contained in terms which are purely imaginary for $b \leq b_c$, and which moreover are vanishing in the limit $\chi \to \infty$.

Since we are mainly interested in the impact-parameter amplitude in Minkowski space we shall extend the result beyond b_c by making use of an appropriate analytic continuation. To justify this procedure from a mathematical point of view we can invoke analyticity in the impact parameter, which allows us to determine the value of the impact-parameter amplitude for $b > b_c$ up to fixing the ambiguity in the choice of the Riemann sheet.

As we have said above, b_c is a branch point for $S_{\text{eff, M}}$, and so we need to specify a prescription in order to go from $b < b_c$ to $b > b_c$. To this extent, we choose the usual "$-i\varepsilon$" prescription, making the substitution $b_c \to b_c - i\varepsilon$. Defining $y = b_c/b$, this prescription amounts to going from $y > 1$ to $y < 1$ passing in the lower half of the complex y-plane, so that the phase of $y - 1$ goes from $-\varepsilon$ to $-\pi + \varepsilon$. We have then

$$\begin{aligned}\sqrt{y^2 - i\varepsilon - 1} &\underset{y>1\to y<1}{\to} -i\sqrt{1-y^2}\,,\\ \operatorname{arccosh} y &\underset{y>1\to y<1}{\to} -i\arccos y\,.\end{aligned} \tag{85}$$

A detailed discussion of the analytic continuation and of the approximations made to obtain an explicit solution can be found in [13]. A dedicated scheme of the analytic continuation is described in Fig. 14.

After analytic continuation, the effective action becomes for $b > b_c$

$$S_{\text{eff, M}} \to \frac{b^2}{2\pi\alpha'_{\text{eff}}\chi}\arccos\frac{b_c}{b} - \frac{2bm}{\chi}\sqrt{1 - \left(\frac{b_c}{b}\right)^2} + 2\pi^2\alpha'_{\text{eff}}m^2\,. \tag{86}$$

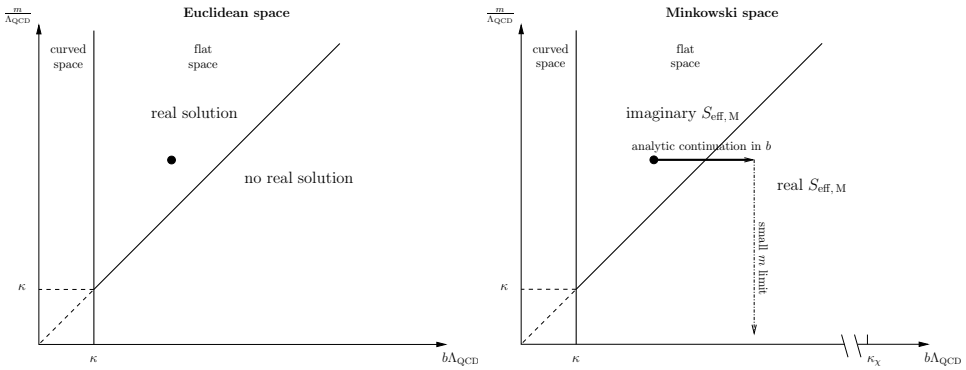

Fig. 14. Analytic continuation in the (b, m) plane (in dimensionless units). Euclidean space (left). Vertical line at $b = R_0 = \kappa\Lambda_{\rm QCD}^{-1}$: separates the region where the relevant geometry is essentially flat ($b\Lambda_{\rm QCD} \geq \kappa$) from the one where the curvature cannot be neglected. Tilted straight line $b\Lambda_{\rm QCD} = m\Lambda_{\rm QCD}^{-1}$: a real solution to the variational problem exists above this line. Together with the vertical line it defines the "wedge" where our approximation is valid. Minkowski spacetime (right). After analytic continuation $\theta \to -i\chi$, which connects the black dots, it is possible to perform a further analytic continuation in b, which allows then to take the small-m limit. The region of $b\Lambda_{\rm QCD}$ relevant to Reggeon exchange extends up to the value $\kappa_\chi = \sqrt{\chi}$.

The effective action is then real at $b > b_{\rm c}$; moreover, for very large $b \gg b_{\rm c}$ the expression simplifies to

$$S_{\rm eff,\,M} \simeq \frac{b^2}{4\alpha'_{\rm eff}\chi} - \frac{4bm}{\chi} + 2\pi^2\alpha'_{\rm eff}m^2 \tag{87}$$

which yields then a Gaussian-like impact-parameter amplitude.

Let us finally compute the Reggeon-exchange amplitude Eq. (47) by performing the Fourier transform of the impact-parameter amplitude, namely

$$\mathcal{A}_{\mathcal{R}}\left(s, t = -q^2\right) \equiv -2is \int d^2b, e^{i\vec{q}\cdot\vec{b}}\, a\left(\vec{b}, \chi\right) = -4i\pi s \int_0^\infty db\, b\, J_0(qb)\; a(b, \chi)\,, \tag{88}$$

where in the last passage we have used azimuthal invariance, and with a small abuse of notation we have denoted $a(\vec{b}, \chi) = a(b, \chi)$.

The impact-parameter amplitude is given by the product of several factors, see *e.g.* the original formula (48), all of which are discussed in [13]. In

an appropriate approximation, it is enough to consider the main contribution coming from the action, namely $e^{-S_{\text{eff, M}}}$ at the saddle point, which up to order $\mathcal{O}(m)$ reads (see also Fig. 15)

$$e^{-S_{\text{eff, M}}} = e^{-\frac{b^2}{4\alpha'_{\text{eff}}\chi}} \left(1 + \frac{4bm}{\chi}\right) + \mathcal{O}\left(m^2\right) . \tag{89}$$

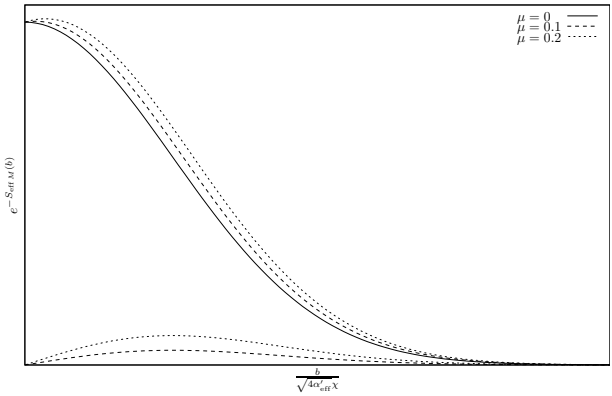

Fig. 15. Impact-parameter amplitude at small m. Plot of the full saddle-point contribution $e^{-S_{\text{eff, M}}}$ in Eq. (89) to the impact-parameter amplitude (upper curves) and of the mass-dependent term alone (lower curves) for different values of $\mu = 8m\sqrt{\alpha'_{\text{eff}}/\chi}$.

We therefore consider the following expression for the Reggeon-exchange amplitude

$$\begin{aligned} \mathcal{A}_{\mathcal{R}}(s,t) &\approx \frac{1}{2\alpha'_{\text{eff}}\chi} \int_0^\infty db\, b\, e^{-\frac{b^2}{4\alpha'_{\text{eff}}\chi}} \left(1 + \frac{4bm}{\chi}\right) J_0(qb) + \mathcal{O}(m^2) \\ &= \mathcal{T}_0(\chi,t) + m\mathcal{T}_1(\chi,t) + \mathcal{O}\left(m^2\right) . \end{aligned} \tag{90}$$

Moreover, in Eq. (90) we have introduced the quantities

$$\begin{aligned} \mathcal{T}_0(\chi,t) &= e^{\alpha'_{\text{eff}}t} , \\ \mathcal{T}_1(\chi,t) &= 8\sqrt{\pi\alpha'_{\text{eff}}}\,\frac{\delta}{\delta\chi}\left[\sqrt{\chi}\tilde{I}_0\left(\alpha'_{\text{eff}}\chi\frac{q^2}{2}\right)\right] , \end{aligned} \tag{91}$$

where $\tilde{I}_n(z) \equiv e^{-z} I_n(z)$, with $I_n(z)$ the modified Bessel functions.

- *First term*
  The first term corresponds to a Regge amplitude with a *linear* Regge trajectory

$$\alpha(t) = \alpha_0 + \alpha_1(t)\,, \qquad \alpha_0(t) = 0\,, \qquad \alpha_1 = \alpha'_{\rm eff} t\,. \tag{92}$$

  This first term is the only one remaining after the limit $m \to 0$. This result was already present in [5], from a direct extrapolation to the zero mass case. The analytic continuation procedure from Euclidean to Minkowski space, derived in [13] thus confirms the conjecture.

- *Second term*
  The second term in (90), see (91), gives for the first time, the small-mass correction to the Regge amplitude due to a small-mass quark in the exchange of a $q\bar{q}$ Regge trajectory. As a first remark, notice that the slope of the amplitude at $t = 0$, given by

$$\frac{\delta \mathcal{A}_{\mathcal{R}}}{\delta t}(s, t = 0) = \alpha'_{\rm eff} \left(\chi + 6m\sqrt{\pi \alpha'_{\rm eff}\chi}\right)\,, \tag{93}$$

  is increased by the effect of the quark mass. Moreover, the dependence of the slope on energy is stronger when $m \neq 0$. These effects are related to the effective increase of the width of the impact-parameter amplitude, which can be seen in Fig. 15.

To uncover the nature of the corresponding Reggeon singularity we compute the Mellin transform of the amplitude. We can conveniently express the Mellin transform as an integral over χ, *i.e.*

$$\mathcal{A}^{(\rm M)}(\omega, t) = \int_0^\infty d\chi e^{-\omega\chi} \mathcal{A}(\chi, t)\,. \tag{94}$$

After a detailed estimate of all contributions, see [13] and putting everything together we find

$$\mathcal{A}^{(\rm M)}(\omega, t) \underset{\omega \to \alpha'_{\rm eff} t}{\simeq} \frac{1 + 8\alpha'_{\rm eff} m t^{\frac{1}{2}}}{\omega - \alpha'_{\rm eff} t} + 4mt^{-\frac{1}{2}} \log \frac{16\alpha'_{\rm eff} t}{\omega - \alpha'_{\rm eff} t}\,. \tag{95}$$

The leading singularity of $\mathcal{A}^{(\rm M)}$ is then a pole at $\omega = \alpha'_{\rm eff} t$, with residue (up to numerical factors)

$$\text{Res} = 1 + 8\alpha'_{\rm eff} t^{\frac{1}{2}} m\,. \tag{96}$$

Moreover, there is a logarithmic branch-point singularity at $\omega = \alpha'_{\text{eff}} t$ due to the second term of $\mathcal{A}^{(\text{M})}$. At $t = 0$ this singularity becomes an algebraic one, since in that case $\mathcal{A}^{(\text{M})} \sim \omega^{-\frac{1}{2}}$ near $\omega = 0$.

Note that, although the nature of the singularity seems more complicated than in the massless case, involving also Regge cuts, the Reggeon trajectory is still linear after the inclusion of terms of order $\mathcal{O}(m)$.

2.4. From Reggeon to Pomeron: the multi-sheet structure of the effective action

The results discussed so far are based on the use of the "$-i\varepsilon$" prescription for the analytic continuation of Eq. (84) from $b < b_{\text{c}}$ to $b > b_{\text{c}}$, leading to Eq. (86) for the Minkowskian effective action. As we have mentioned in the previous section, it is possible that the whole multi-sheet structure of the Minkowskian effective action is physically relevant. A careful analysis shows that in the most general case the analytic continuation of Eq. (84) from $b < b_{\text{c}}$ to $b > b_{\text{c}}$ leads to

$$\begin{aligned} &S_{\text{eff, M}}|_{b<b_{\text{c}}} \to S^{(\pm,n)}_{\text{eff, M}}|_{b>b_{\text{c}}} \\ &= \pm \left\{ \frac{b^2}{2\pi\alpha'_{\text{eff}}\chi} \arccos\frac{b_{\text{c}}}{b} - \frac{2bm}{\chi}\sqrt{1-\left(\frac{b_{\text{c}}}{b}\right)^2} \right\} + 2\pi^2\alpha'_{\text{eff}} m^2 + \frac{nb^2}{\alpha'_{\text{eff}}\chi}\,, \end{aligned} \tag{97}$$

with $n \in \mathbb{Z}$, depending on the specific prescription chosen for the analytic continuation, *i.e.*, on the path in the complex plane along which the analytic continuation is performed. Here, $\arccos x$ denotes the principal determination of the inverse cosine function, *i.e.*, $\arccos x \in [0, \pi]$. The last term in Eq. (97) comes from the analytic continuation of this function, $\arccos x \to \pm\arccos x + 2n\pi i$, along paths in the complex plane which wind a certain number of times around -1.

As we have already said, we do not have a precise mathematical argument which would select a specific prescription, and so one of the possibilities $S^{(\pm,n)}_{\text{eff, M}}|_{b>b_{\text{c}}}$ for the Minkowskian effective action. As a consequence, we have to use physical arguments in order to discriminate among the various possibilities. A first requirement, related to the unitarity bound on the impact-parameter amplitude, is that the resulting amplitude vanishes for $b \to \infty$. The simplest choice satisfying this requirement is the "$-i\varepsilon$" prescription, *i.e.*, $S^{(+,0)}_{\text{eff, M}}|_{b>b_{\text{c}}}$, but it is clearly not the only one. A second reasonable requirement is that the last term in Eq. (97) may be interpreted as a correction to a given basic amplitude for Reggeon exchange. Stated differently, we ask that setting $n = 0$ we obtain a physically acceptable quantity. These two requirements restrict the possibilities to $S^{(+,n)}_{\text{eff, M}}|_{b>b_{\text{c}}}$ with $n \in \mathbb{N}$.

We will make now the following working hypothesis: we will assume that all the physically sensible choices $S^{(+,n)}_{\mathrm{eff,M}}|_{b>b_c}$, $n \in \mathbb{N}$, contribute to the Reggeon-exchange amplitude. The determination of the full contribution of each of the admissible terms to the scattering amplitude appears to be a difficult task, which would require the knowledge of their relative weights in the functional integral Eq. (48) (after analytic continuation to Minkowski space-time). However, from their analytical structure and formal properties, the new contributions can be put into a relation with physical processes which are expected to take place in meson–meson scattering at high energy.

Indeed, one finds that each contribution to the impact-parameter amplitude is proportional to the following factorised expression

$$\exp\left\{-S^{(+,n)}_{\mathrm{eff,M}}\right\} = \exp\{-S_{\mathrm{eff,M}}\} \times \left[\exp\left\{-\frac{b^2}{\alpha'_{\mathrm{eff}}\chi}\right\}\right]^n , \tag{98}$$

where $S_{\mathrm{eff,M}} \equiv S^{(+,0)}_{\mathrm{eff,M}}$ is the effective action given explicitly in Eq. (86), corresponding to the Reggeon-exchange amplitude discussed in the previous section, and where for notational simplicity we have dropped the subscript $|_{b>b_c}$. Going from impact-parameter to transverse momentum space via Fourier transform, and ignoring possible b-dependent prefactors, which can be treated as discussed in the previous subsection, one obtains for each component

$$\begin{aligned}
\mathcal{A}^{(+,n)}\left(s, t=-\vec{q}^{\,2}\right) &\equiv \int d^2b\, e^{i\vec{q}\cdot\vec{b}}\, \exp\left\{-S^{(+,n)}_{\mathrm{eff,M}}\right\} \\
&= \int d^2b\, e^{i\vec{q}\cdot\vec{b}}\, \exp\{-S_{\mathrm{eff,M}}\} \left[\exp\left\{-\frac{b^2}{\alpha'_{\mathrm{eff}}\chi}\right\}\right]^n \\
&= i^n \mathcal{A}^{(+,0)}(s,t) \otimes \mathcal{A}^{\otimes n}_{\mathrm{el}}(s,t)\,,
\end{aligned} \tag{99}$$

where $\otimes$ is the sign of a *convolution*, defined here as

$$f(t) \otimes g(t) \equiv \frac{1}{2s} \int \frac{d^2k}{(2\pi)^2}\, f\left(-\left(\vec{q}-\vec{k}\right)^2\right) g\left(-\vec{k}^{\,2}\right), \qquad t = -\vec{q}^{\,2}\,, \tag{100}$$

and where the amplitudes $\mathcal{A}^{(+,0)}$ and $\mathcal{A}_{\mathrm{el}}$ are given by

$$\begin{aligned}
\mathcal{A}^{(+,0)}(s,t) &= \int d^2b\, e^{i\vec{q}\cdot\vec{b}}\, \exp\{-S_{\mathrm{eff,M}}\}\,, \\
\mathcal{A}_{\mathrm{el}}(s,t) &= -i2s \int d^2b\, e^{i\vec{q}\cdot\vec{b}} \exp\left\{-\frac{b^2}{\alpha'_{\mathrm{eff}}\chi}\right\} = -2i\pi s\ \alpha'_{\mathrm{eff}}\chi e^{\frac{\alpha'_{\mathrm{eff}}t}{4}\chi}\,.
\end{aligned} \tag{101}$$

The physical interpretation of the resulting convolution (99) becomes quite clear when remarking that the amplitude $\mathcal{A}_{\mathrm{el}}(s,t)$ given by Eq. (101) is

equal (up to prefactors) to the one obtained for elastic dipole–dipole scattering within the same formalism in Ref. [4]. This means that the various components $\mathcal{A}^{(+,n)}(s,t)$ represent the contribution of multiple elastic rescattering interaction between the colliding mesons, occurring together with the $q\bar{q}$-Reggeon exchange previously discussed, which corresponds to the amplitude $\mathcal{A}^{(+,0)}(s,t)$. We find that such elastic contributions are independent of the quark mass, as it is expected, and moreover of Regge-pole type, with Regge trajectory $\alpha_{\rm el}(t) = \alpha_{0\,\rm el} + \alpha'_{\rm el} t$. As already noticed in [3], the "Regge slope" $\alpha'_{\rm el} = \alpha'_{\rm eff}/4$ of the elastic amplitude (101) is one-fourth of the one obtained in the case of $q-\bar{q}$ exchange, and the "Regge intercept" is $\alpha_{0\,\rm el} = 1$ (up to an intercept increase due to fluctuations, see [16]).

From a phenomenological point of view, such contributions are expected to come from the long interaction time allowed by the softness of the interactions at strong coupling in QCD (although a complete theoretical derivation is not yet available). We see here that they may appear in the gauge/gravity framework in relation with the multi-sheet structure of the effective action, if one assumes that all the sheets which are physically sensible (in the sense discussed above) contribute to the scattering amplitude. Although a satisfactory mathematical justification of this assumption is lacking at the moment, a possible origin of these extra contributions is the following. When formulated in terms of the variable $\varphi(s)$, the Euclidean variational problem is invariant under the reparameterisation $\varphi(s) \to \varphi(s) + 2n\pi i$. On the other hand, the expression Eq. (71) for the Euclidean effective action is not: while it is obviously possible to write it in an explicit reparameterisation-invariant form, in doing so one would lose analyticity in $\tilde{\varphi}$. Since an analytic expression is required in order to go from Euclidean to Minkowski space, one has to impose a "gauge choice" (*e.g.*, $\mathrm{Im}\varphi(s) = 0$), and use the corresponding expression for the Euclidean effective action (which in this case would be Eq. (71)). As a result, it is possible that the completely *equivalent* choices $\varphi(s) + 2n\pi i$ in Euclidean space are mapped into *different* solutions of the corresponding variational problem in Minkowski space, each one contributing to the path integral a quantity proportional to expression Eq. (98). This possibility is currently under investigation.

The initial papers and the general method followed in this work comes from a fruitful long-term collaboration with Romuald Janik, whom I warmly thank. The new material is due to a collaboration with Matteo Giordano (*cf.* Ref. [13]) and with him and Shigenori Seki (*cf.* Ref. [6]). Many thanks to them. It is my pleasure to thank Michał Praszałowicz and the Cracow theory group for hospitality and the excellent atmosphere of the Zakopane School.

REFERENCES

[1] P. Di Vecchia, A. Schwimmer, *Lect. Notes Phys.* **737**, 119 (2008) [arXiv:0708.3940 [physics.hist-ph]].

[2] J.M. Maldacena, *Adv. Theor. Math. Phys.* **2**, 231 (1998) [*Int. J. Theor. Phys.* **38**, 1113 (1999)] [arXiv:hep-th/9711200]; S.S. Gubser, I.R. Klebanov, A.M. Polyakov, *Phys. Lett.* **B428**, 105 (1998) [arXiv:hep-th/9802109]; E. Witten, *Adv. Theor. Math. Phys.* **2**, 253 (1998) [arXiv:hep-th/9802150].

[3] R.A. Janik, R.B. Peschanski, *Nucl. Phys.* **B565**, 193 (2000) [arXiv:hep-th/9907177].

[4] R.A. Janik, R.B. Peschanski, *Nucl. Phys.* **B586**, 163 (2000) [arXiv:hep-th/0003059].

[5] R.A. Janik, R.B. Peschanski, *Nucl. Phys.* **B625**, 279 (2002) [arXiv:hep-th/0110024].

[6] M. Giordano, R. Peschanski, S. Seki, arXiv:1110.3680 [hep-th].

[7] N. Drukker, D.J. Gross, H. Ooguri, *Phys. Rev.* **D60**, 125006 (1999) [arXiv:hep-th/9904191].

[8] L.F. Alday, J.M. Maldacena, *J. High Energy Phys.* **0706**, 064 (2007) [arXiv:0705.0303 [hep-th]].

[9] M. Kruczenski, *J. High Energy Phys.* **0212**, 024 (2002) [arXiv:hep-th/0210115].

[10] S.G. Naculich, H.J. Schnitzer, *Nucl. Phys.* **B794**, 189 (2008) [arXiv:0708.3069 [hep-th]].

[11] E. Barnes, D. Vaman, *Phys. Rev.* **D81**, 126007 (2010) [arXiv:0911.0010 [hep-th]].

[12] E. Witten, *Adv. Theor. Math. Phys.* **2**, 253 (1998) [arXiv:hep-th/9802150]; *Adv. Theor. Math. Phys.* **2**, 505 (1998) [arXiv:hep-th/9803131].

[13] M. Giordano, R. Peschanski, *J. High Energy Phys.* **1110**, 108 (2011) [arXiv:1105.6013 [hep-th]]; M. Giordano, R. Peschanski, S. Seki, arXiv:1110.3680 [hep-th].

[14] O. Nachtmann, *Ann. Phys.* **209**, 436 (1991); For a general review, see O. Nachtmann, *High Energy Collisions and Nonperturbative QCD*, in *Perturbative and Nonperturbative Aspects of Quantum Field Theory*, Proceedings of the 35-th International University School of Nuclear and Particle Physics, 2–9 Mar 1996, Schladming, Austria, ed. H. Latal, W. Schweiger, Springer-Verlag, Berlin, Heidelberg 1997, p. 49 [arXiv:hep-ph/9609365]; in *Lectures on QCD: Applications*, ed. H.W. Griesshammer, F. Lenz, D. Stoll, Springer-Verlag, Berlin, Heidelberg 1997, p. 1.

[15] D.J. Gross, H. Ooguri, *Phys. Rev.* **D58**, 106002 (1998) [arXiv:hep-th/9805129].

[16] R.A. Janik, *Phys. Lett.* **B500**, 118 (2001) [arXiv:hep-th/0010069].